NASA TM X-120

TECHNICAL MEMORANDUM
X-120

THE LOW-SPEED STATIC LONGITUDINAL AND LATERAL CHARACTERISTICS OF A DELTA-WING MODEL WITH FIXED AND FREE-FLOATING CANARD SURFACES

By William I. Scallion and Michael D. Cannon

Langley Research Center
Langley Field, Va.

NATIONAL AERONAUTICS AND SPACE ADMINISTRATION

WASHINGTON October 1959

[redacted]

Todd

copy #1

NATIONAL AERONAUTICS AND SPACE ADMINISTRATION

TECHNICAL MEMORANDUM X-120

THE LOW-SPEED STATIC LONGITUDINAL AND LATERAL CHARACTERISTICS OF A DELTA-WING MODEL WITH FIXED AND FREE-FLOATING CANARD SURFACES*

By William I. Scallion and Michael D. Cannon

SUMMARY

An investigation was conducted in the Langley full-scale tunnel to determine the static longitudinal and lateral characteristics of a delta-wing canard model with canard surfaces fixed and free floating. The model was tested with canard surfaces having areas of 15 and 20 percent of the wing area and with two vertical-tail configurations, a single vertical tail mounted on the center line of the body and twin vertical tails mounted outboard on the wing. Limited tests were also made to determine the effect of body nose shape and of a strake on the model lateral characteristics.

The results indicated that the longitudinal trim characteristics of the model with the free-floating canard surface were superior to those with the canard surface fixed. For example, for a corresponding degree of static stability, the free-floating canard-surface arrangement could be trimmed to a lift coefficient of 1.3, whereas the fixed canard-surface arrangement could be trimmed to a lift coefficient of only 0.8. If the usable angle of attack was limited to about 14° because of ground clearance at take-off and landing, the trim lift coefficient at these angles would be 0.76 and 0.62 for the free-floating canard-surface and fixed-canard-surface configurations, respectively. The fixed-canard-surface arrangement with twin vertical tails mounted outboard on the wing was directionally stable over the entire lift-coefficient range that could be trimmed. The maximum usable trim lift coefficient of the model with the free-floating canard surface was limited by directional stability to a value of 1.2.

*Title, Unclassified.

INTRODUCTION

Previous investigations (refs. 1 and 2, for example) have shown that canard configurations can provide considerable advantages in performance at supersonic speeds over that of the tailless configuration or configurations with rearward horizontal tails. The opposite trend, however, has been evident in the low-subsonic-speed range (refs. 3 and 4), wherein the problem of canard-surface stall and the detrimental effect of the long body nose lengths on the directional characteristics at high attitudes placed severe penalties on the landing and take-off performance of canard arrangements. The advantages of canard arrangements at supersonic speeds, however, were deemed sufficiently important to justify further evaluation of the low-speed characteristics of a canard configuration in the Langley full-scale tunnel. A modified delta-wing plan form was chosen because the delta was considered a representative high-speed plan form for which abundant high-speed information existed.

One method of attaining higher trim lift coefficients with a canard control was studied in reference 5 in which the canard control was free floating. The free-floating canard surface permitted a more rearward center-of-gravity location than a fixed canard surface, and therefore the trim capability of the canard surface was increased. This concept was extended in the present investigation to include an evaluation of the longitudinal trim capability of the free-floating canard surface in conjunction with wing trailing-edge flaps and flap blowing for high lift.

The longitudinal and lateral characteristics of the model were obtained with the canard surfaces fixed and free floating and with two vertical-tail arrangements. The effects of the body nose shape and a nose strake on the model characteristics were also briefly studied. The test Reynolds number was 2.3×10^6 and the Mach number was 0.10.

The data are utilized for comparisons of three possible canard-surface arrangements: canard surface fixed, canard surface free floating, and a composite canard-surface arrangement having a center-of-gravity location compatible with a fixed canard surface at supersonic speeds and a free-floating-canard surface at low subsonic speeds.

COEFFICIENTS AND SYMBOLS

The longitudinal aerodynamic data are referred to the stability system of axes and the lateral data are referred to the body system of axes as shown in figure 1. The coefficients and symbols used are defined as follows:

C_D drag coefficient, $\frac{\text{Drag}}{q_\infty S}$

C_L lift coefficient, $\frac{\text{Lift}}{q_\infty S}$

$C_{L,max}$ maximum lift coefficient

$C_{L,trim}$ trim lift coefficient

ΔC_L increment in lift coefficient

C_l rolling-moment coefficient, $\frac{\text{Rolling moment}}{q_\infty Sb}$

C_m pitching-moment coefficient, $\frac{\text{Pitching moment}}{q_\infty S\bar{c}}$

C_n yawing-moment coefficient, $\frac{\text{Yawing moment}}{q_\infty Sb}$

C_Y side-force coefficient, $\frac{\text{Side force}}{q_\infty S}$

C_μ blowing-jet momentum coefficient

$\frac{dC_m}{dC_L}$ rate of change of pitching-moment coefficient with respect to lift coefficient

C_{l_β} $\frac{\partial C_l}{\partial \beta}$ (slopes measured from $\beta = -5^\circ$ to 0° or $\beta = 0^\circ$ to 5°), per degree

C_{n_β} $\frac{\partial C_n}{\partial \beta}$ (slopes measured from $\beta = -5^\circ$ to 0° or $\beta = 0^\circ$ to 5°), per degree

C_{Y_β} $\frac{\partial C_Y}{\partial \beta}$ (slopes measured from $\beta = -5^\circ$ to 0° or $\beta = 0^\circ$ to 5°), per degree

b	wing span, ft
$\bar{c}$	mean aerodynamic chord, ft
D	drag force, lb
M	Mach number
q_∞	free-stream dynamic pressure, lb/sq ft
S	wing area, sq ft
V	velocity, knots
V_{stall}	velocity at $C_{L,max}$
x	longitudinal distance from leading edge of the mean aerodynamic chord to center of gravity, positive rearward, ft
α	model angle of attack, deg
β	model angle of sideslip, deg
i_t	canard-surface incidence, relative to the model center line, deg
α_t	canard-surface floating angle, relative to free stream, deg
δ_f	angle of flap deflection with respect to wing chord line, deg

Model components:

WF	wing body
V_1	body-mounted center vertical tail
V_2	wing-mounted twin vertical tails
H_1	0.20S delta canard surface
H_2	0.15S delta canard surface
N_1	body nose upright
N_2	body nose inverted

s_1 body nose strake

s_2 body nose strake cut out for canard-surface installation

MODEL AND TESTS

Model

The geometric details of the model used in this investigation are given in figures 2 and 3, and a photograph of the model is shown on figure 4. The wing was mounted on the model center line (fig. 2) and had a delta plan form with 5 percent of the total area removed at the tips. The wing aspect ratio was 1.47, and the airfoil sections parallel to the plane of symmetry were NACA 65_A006. The wing was equipped with a constant-chord trailing-edge flap that was hinged at the 0.88 root-chord station. A full-span blowing slot was located in the wing shroud just ahead of the flap in order to provide boundary-layer control on the flap when it was deflected.

The body fineness ratio was 10.83; and as shown in figure 2, the body cross section rearward of section D-D (body station 75.6) was circular, and the body ahead of this station was shaped to provide a minimum gap at the canard-surface—body juncture. The nose section forward of station 75.6 could be rotated 180° about the nose center line (fig. 2) so that two vertical locations for the canard surfaces were obtained; one with the canard surface on the wing chord plane (nose upright, N_1), and one with the canard surface $0.07\bar{c}$ below the wing chord plane (nose inverted, N_2).

The two canard surfaces (hereinafter referred to as canards) used in the tests are shown in figures 2 and 3. One canard, which had an area of 15 percent of the total wing area, was a 1/4-inch-thick aluminum plate with a rounded leading edge and a chamfered trailing edge. The other canard, which had an area of 20 percent of the total wing area, was an aluminum insert overlaid with balsa wood and fiber glass forming an NACA 65A003 airfoil section. The canard hinge line was located $1.45\bar{c}$ ahead of the wing 27.5 percent $\bar{c}$ station, and the canards were statically balanced so that data could be obtained with the canards either locked at a fixed incidence or free floating with the incidence set by using split-flap-type tabs mounted on the canard.

Two vertical-tail arrangements were provided (fig. 2). A center tail (designated as V_1) was mounted on the body, and twin tails (designated as V_2) were mounted outboard on the wing at the 0.85 semispan

station. The total areas of the two tail arrangements were approximately equal and were about 21 percent of the total wing area. In addition, the nose strake shown in figure 3 was provided for use in a limited part of the program. The strake was a continuous sheet-metal strip, and the span was equal to one-tenth of the maximum body diameter. As shown in figure 3, the strake was cut out to allow for installation of the canards and the same cutout was used in conjunction with both the 0.15S and 0.20S canards.

Tests

A complete listing of the model configurations and the range of angle of sideslip for which they were tested are given in table I. The initial longitudinal tests were conducted on the model with the 0.15S and 0.20S canards fixed at incidence angles ranging from -30° to 30° with the full-span wing flaps deflected 0° and 10° to determine the effect of canard size and moderate flap deflection on the stability and trim characteristics. Tests were also made with the 0.20S canard fixed and with the center vertical tail (V_1) replaced by the twin vertical tails (V_2).

The main objective of the longitudinal tests was to determine the trim capability of the 0.20S free-floating canard in combination with several wing-flap arrangements used to obtain increased lift at a given angle of attack. These tests were conducted on the model with the 0.20S free-floating canard in conjunction with inboard-wing-flap deflections of 35° and 45° with and without high-pressure blowing boundary-layer control and full-span flap deflections of 10° and 20° without blowing. The range of wing-flap arrangements that could be trimmed by the free-floating canard was fairly well defined by the aforementioned tests.

Sideslip tests were conducted at $\beta = -5^\circ$, 0°, and 5° to determine the effect of the model nose in upright and inverted positions and the nose strake on the static lateral characteristics of the model with the center vertical tail and the canard control removed. These tests were repeated with the 0.15S and 0.20S fixed canards installed. Additional tests were made with the 0.20S fixed canard in combination with the twin vertical tails mounted outboard on the wing (V_2) to determine the effect of vertical-tail arrangement on the static lateral characteristics of the model. The canard-incidence range in these tests was -20° to 10°, and this range was sufficiently large to permit derivation of the model characteristics in sideslip with the canard free floating.

Aerodynamic forces and moments were measured for an angle-of-attack range of -1.8° to 34.8° at a test Reynolds number of 2.3×10^6 and a Mach number of 0.10. Tunnel jet-boundary and buoyancy corrections were calculated and found to be negligible, and therefore they were not applied.

All the tests were made without fixed transition on the model body and aerodynamic surfaces.

RESULTS AND DISCUSSION

Longitudinal Characteristics

The basic results of the longitudinal investigation of the model with the 0.15S and 0.20S canards fixed and with the canard removed are presented in figures 5 to 10. For comparative purposes, the data for the fixed canard arrangements (figs. 5 to 9) are shown for center-of-gravity locations chosen so that the minimum longitudinal stability dC_m/dC_L was zero for the model with flaps neutral. The results obtained with the 0.20S free-floating canard are presented for a center-of-gravity location of $0.275\bar{c}$ in figures 11 to 16. Figures 12 to 16 show the basic results of the investigation to define the range of wing-flap arrangements that could be trimmed by the 0.20S free-floating canard. As shown in figure 12, the model could be trimmed to maximum lift with the inboard flaps deflected 45° without boundary-layer control. The increment in C_m between the trimmed and untrimmed curves for this case indicates capability of also trimming the model with partial-span flaps deflected 35° with blowing boundary-layer control. The trim capability of the canard was insufficient to trim the moments produced by blowing at the higher flap deflections (45°) where blowing would be more profitably used. With an improvement in the canard lifting efficiency, longitudinal trim with higher flap deflections and boundary-layer control might be obtained.

The test results also showed that the model with the full-span flaps deflected 20° without blowing could be trimmed with the free-floating canard (fig. 16). A comparison of the data on figures 12 and 13 shows that the lift effectiveness of the 35° inboard flap with blowing and the 20° full-span flap was generally greater than that of the 45° flap without blowing. The 20° full-span flap arrangement had a lower pitching-moment coefficient than the 35° inboard flap, and this arrangement was chosen as a representative flapped wing configuration for detailed study.

The results of the longitudinal investigation of the model with the canards fixed and free floating are presented in summary form in figures 17 to 22. Three canard-airplane arrangements are derived from the basic data that are assumed to be practical aircraft arrangements, consisting of canard fixed, canard free floating, and a composite arrangement in which the canard was free floating at subsonic speeds with a center-of-gravity location compatible with the canard fixed at supersonic speeds.

The form of these summary figures provides a convenient examination of the center-of-gravity-position requirements dictated by longitudinal stability and canard trim capabilities for the three possible arrangements and also provides a basis for examining the resulting directional, lateral problems in a later section of this paper. The curves on figures 17 to 22 represent the maximum trim capability of the canard as limited by canard stall for a given center-of-gravity location. The flat portion of the curves where the variation of $C_{L,trim}$ with $x/\bar{c}$ is zero, represents the maximum lift coefficient of the model. The symbols on the curves indicate the minimum degree of longitudinal stability within the trim lift-coefficient range for the given center-of-gravity location as determined from the C_m plotted against C_L curves of the basic data curves on figures 5 to 10 and similar curves for other center-of-gravity locations. Scales on the right sides of the figures are nonlinear and are presented to show the appropriate angles of attack for a given lift coefficient.

Canard fixed.- The low-speed-longitudinal-trim characteristics of the model with fixed canard controls as affected by canard-size, flap deflection, and vertical-tail arrangement are shown in figures 17 to 19.

As shown on figure 17, the maximum trim lift coefficient attainable with the canards fixed depended upon the center-of-gravity location. The maximum trim lift coefficient in any case for center-of-gravity locations for neutral or positive stability would be limited by canard stall to values below the wing maximum lift coefficient. For example, the maximum trim lift coefficient of the model with the 0.20S canard and having neutral stability would be approximately 1.0, and a more forward center-of-gravity location for increased stability would have a corresponding decrease in maximum trim lift coefficient. For the same degree of stability, figure 17 shows that the trim lift effectiveness of the model with the 0.20S canard was only slightly better than with the 0.15S canard. The greater effectiveness of the 0.20S canard was offset by the shorter tail moment arm resulting from the more forward center-of-gravity location required for the larger canard.

Figure 18 shows that the negative increment in pitching-moment coefficient associated with just 10° full-span flap deflection materially reduced the trim lift coefficient attainable with the 0.20S canard. The angle of attack for a given lift coefficient, however, was reduced about 3.5° by the 10° flap deflection; and for applications for which the ground attitude for an airplane is limited to about 12° to 14°, the use of flaps at low deflection would provide some gain in trim lift coefficient.

A comparison of the longitudinal trim characteristics of the model with the single and twin vertical-tail arrangements with the 0.20S canard are shown in figure 19. The longitudinal trim capability of the model

with the twin vertical tails was reduced about a ΔC_L of 0.1 from that with the single vertical tail. This effect was shown in references 6 and 7 to be associated with the interference of the wing-mounted tails on the wing flow field, and suggests further study to determine suitable tail locations without penalizing the longitudinal characteristics of the configuration.

Canard free floating.- The longitudinal trim characteristics of the model with the 0.20S free-floating canard are summarized in figure 20. The curve on figure 18 for the fixed canard ($\delta_f = 0^\circ$) is also repeated on figure 20 for comparison with the free-floating-canard characteristics. This comparison shows that for a given center-of-gravity location, a large difference between the trim capability of the fixed- and free-floating-canard arrangements existed. On the basis of the fact that the untrimmed pitching moment of the model without a canard is fixed for a specific center-of-gravity location, the canard lift required to overcome this moment is the same for either case, and the difference on figure 20 indicates a reduced free-floating-canard lift effectiveness. The reduced effectiveness was caused by using a tab to obtain canard floating angles. Increased free-floating-canard effectiveness could be obtained by a more efficient tab arrangement than the trailing-edge split flap used in this investigation, and effectiveness equal to that of the fixed canard is theoretically possible by synthetically floating the canard with a sensing device to deflect the canard. On the basis of the preceding discussion, the trim capability of the free-floating canard as presented herein is believed to be conservative.

As can be seen on figure 20, the model with the flaps neutral could be trimmed to the maximum lift coefficient with adequate longitudinal stability for a wide range of center-of-gravity locations between 17 and 32 percent $\bar{c}$. The increase in trim lift coefficient over that of the fixed-canard arrangement with neutral stability amounted to about 0.32; however, the gain in lift would require a corresponding increase in angle of attack of approximately 11°. In practice the angle of attack of highly swept, low-aspect-ratio configurations is usually limited to angles a great deal less than those for maximum lift, and where this is the case, the potential trim lift of the free-floating-canard arrangement with flaps neutral would not be realized. As shown on figure 20, the real advantage of the free-canard arrangement was the ability to trim to maximum lift with the flaps deflected 10° and 20°, where, for a given trim lift coefficient, the angle of attack was reduced approximately 4° and 7°, respectively, over that of the model with flaps neutral. At $\alpha = 14^\circ$ the trim lift coefficient for the model with neutral flaps was 0.64 for a center-of-gravity range of 32 percent $\bar{c}$. The $C_{L,trim}$ at this angle of attack was increased to 0.85 and 0.97 with 10° and 20° of flaps, respectively. The center-of-gravity range with the flaps deflected 10° was 14.5 percent $\bar{c}$; however, because of the more rearward center-of-gravity

location required for trim, the center-of-gravity range of the model with the flap deflected 20° was reduced to about 2 percent $\bar{c}$. As mentioned previously, an increase in the free-floating-canard lifting efficiency would increase the center-of-gravity range at a given trim lift coefficient for both the 10° and 20° flap deflections.

The effect of locating the vertical tails outboard on the wing on the model with the free-floating canard is shown on figure 21. The net result was average reduction of $C_{L,trim}$ for given center-of-gravity locations of 0.1 and 0.25 for configurations with the flaps neutral and with flaps deflected 10°, respectively. The configuration with flaps deflected 20° could not be trimmed with center-of-gravity locations that provided longitudinal stability. The configuration with flaps deflected 10° attained a trim lift coefficient of 0.77 for a center-of-gravity range of 6 percent $\bar{c}$ at $\alpha = 14°$. The average reduction in angle of attack produced by a flap deflection of 10° was about 5° more than with the flaps neutral.

Composite canard arrangement.- The preceding discussion has shown that the free-floating canard was superior to the fixed canard as a low-speed trimming device; however, this might not be the case at supersonic Mach numbers. As indicated in reference 8, a decrease in the free-floating canard effectiveness with increasing Mach number would be expected for a canard with a trailing-edge-flap type control. The severity of this factor and the possibility of flutter of the free-floating canard at transonic speeds may lead to the consideration of a third canard arrangement in which the canard was free floating for low-speed flight and fixed at supersonic speeds. The apparent advantage of a composite arrangement over that of the fixed canard would be the ability to reduce the trim drag at supersonic speeds by utilizing a slightly more rearward center-of-gravity location and by maintaining longitudinal stability at low speeds by floating the canard. The location of the center of gravity would depend upon the longitudinal stability desired at the operational Mach number of the aircraft, and this center-of-gravity location would in turn determine the low-speed stability and trim characteristics with the free-floating canard. As shown on figure 2 of reference 2, there is a wide variation in longitudinal stability with Mach number; therefore, the low-speed characteristics resulting from choosing one design Mach number and degree of stability would be different for other values of Mach number and stability. Examples of the low-speed longitudinal trim characteristics of two composite canard arrangements based on a combination of the results of reference 2 for a delta-wing canard configuration and the results of the present investigation are indicated on figure 22. Two design Mach numbers, 1.5 and 2.0, were chosen, and a value of $dC_m/dC_L = -0.03$ was chosen for both cases. It can be seen in figure 2 of reference 2 that the difference in stability between

subsonic speeds and Mach numbers of 1.5 and 2.0 are -0.07 and -0.035, respectively, and the center-of-gravity locations for the two examples shown in figure 22 were chosen accordingly.

It can be noted in figure 22 that the center-of-gravity locations resulting from the required stability at supersonic Mach numbers produced a large degree of stability at low speeds with the canard free floating and that the maximum trim lift coefficients were consequently fairly low, about 0.7 and 0.8. It can also be seen from the figure that if a configuration in which the canard was fixed throughout the speed range was used, a somewhat higher value of the maximum trim lift coefficient could be obtained, for example, $C_{L,trim} = 0.9$ with $dC_m/dC_L = -0.02$. The example cited above, however, would require a more forward center-of-gravity location for stability at low speeds, and consequently would have a higher degree of stability along with a greater trim penalty than that of the composite arrangement at supersonic speeds. Additionally, if the landing and take-off attitudes were limited because of ground clearance to angles less than approximately 16°, the differences in trim lift coefficient for landing or take-off between the fixed and composite canard arrangements would be negligible.

From the preceding discussion of the longitudinal trim characteristics of the model, it has been shown that of the three arrangements considered, the free-floating canard had the highest trim capability. The trim capability of the fixed or composite canard arrangements was limited because of the more forward center-of-gravity location necessary for longitudinal stability. One advantageous feature common for both the composite canard at low speeds (with the canard free floating) and the free-floating canard is the elimination of canard stall, by limiting the control-tab power to deflect the canard to angles below those for stall.

Lateral Characteristics

The basic results of the investigation to determine the effect of body nose shape, nose strakes, canards, and vertical-tail arrangement on the static lateral characteristics of the model are presented in figures 23 to 29. The arrangements considered to have the better directional characteristics are compared on figure 30 for center-of-gravity locations considered usable for the fixed-canard and free-floating-canard arrangement previously discussed in connection with the longitudinal characteristics.

Basic data.- As can be seen on figure 23, the directional stability of the model without canards above $C_L = 0.5$ was greatly reduced when the unsymmetrical nose section of the body was inverted. The reduction

in directional stability accompanied by a large decrease in C_{Y_β} suggested that there was an increase in the side-force load on the inverted nose (N_2). Addition of a strake to the model with the upright nose (N_1) produced a large increase in the directional stability of the model without canards (fig. 24); however, with the canards installed (figs. 25 and 26), the strakes were relatively ineffective. The canards had about the same effect in increasing C_{Y_β} as strakes alone; however, the possible reduction in the loading on the nose in this case was probably offset by an adverse sidewash at the vertical tail. (See refs. 9 and 10.) Addition of the canards tended to reduce the directional stability of the model with the nose upright (figs. 25 and 26); however, the opposite trend was shown with the nose inverted (fig. 27). The causes of the effects pointed out in the above discussion could not be definitely established by this investigation, and it was apparent that more detailed investigations (pressure distributions and the flow field of the body and vertical tail) would be necessary to attain a better understanding of the aforementioned phenomena.

When the data of figure 25 were computed for center-of-gravity locations, considered useful from the longitudinal standpoint, they showed that the model with the center vertical tail with the 0.20S canard fixed or free floating was directionally unstable above $C_L = 0.8$. This result was attributed in part to the aforementioned adverse sidewash effects of the model nose and canard-surface flow field on the center vertical tail. A comparison of the model directional characteristics with the center vertical tail with those with the twin vertical tails (fig. 28) shows that the directional stability of the twin-vertical-tail arrangement was considerably better than that of the single-vertical-tail arrangement, and directional stability was maintained to maximum lift.

Trimmed directional characteristics, canard fixed and canard free.- The trimmed directional stability characteristics of the model with twin vertical tails with the 0.20S canard fixed and free floating are compared in figure 30.

Although the longitudinal data indicated that somewhat better longitudinal trim capability was obtained on the model with the center vertical tail, the lateral data showed that the directional stability of this configuration was insufficient for the lift coefficient range for which it could be trimmed. On the basis of the results of this investigation, the configuration with the twin vertical tails would have the best combination of longitudinal and lateral characteristics, and for this reason the twin-vertical-tail configuration was used for the comparison. The center-of-gravity locations given for the curves on the upper half of figure 30 were chosen for a small degree of longitudinal stability for each case, $dC_m/dC_L = -0.02$ and -0.01 at $\delta_f = 0^\circ$ for the canard fixed and canard free, respectively.

As can be seen on the upper half of figure 30, the fixed-canard arrangement was directionally stable up to the highest trim lift coefficient attainable ($C_{L,trim} = 0.82$); however, the canard-free arrangement with the flaps neutral was directionally unstable at a trim lift of 0.7, a value considerably lower than that to which this arrangement could be longitudinally trimmed. The reduced stability of the canard-free arrangement was caused by a combination of the shorter vertical-tail moment arm and the low to negative canard deflections required for trim that resulted from the far rearward center-of-gravity location ($0.275\bar{c}$). The directional stability of the canard-free arrangement could be increased by having a more forward center-of-gravity location, and the result of a 6.5 percent $\bar{c}$ forward shift of the center of gravity is shown on the lower half of figure 30. With the center of gravity at $0.21\bar{c}$, the lift coefficient for zero directional stability was increased to 0.90. In addition to the direct effect of the more forward center-of-gravity location (an increased vertical-tail moment arm), an indirect effect was produced by causing a small positive increase in the canard deflection required for trim, and as shown on figure 29, this also increased the directional stability. At the more forward center-of-gravity location ($0.21\bar{c}$), deflection of the flaps 10° increased the trim lift coefficient for directional stability to approximately 1.2. As can be seen on figure 21 the $0.21\bar{c}$ center-of-gravity location was about the optimum location for the free-floating canard arrangement ($\delta_f = 10^\circ$) because a more forward center-of-gravity location would result in a reduced trim lift.

Low-Speed Performance Characteristics

The low-speed level-flight performance characteristics of two canard airplanes that were assumed to have the characteristics of the model of this investigation with the canard fixed and the canard free floating are compared in figure 31. A landing wing loading of 50 pounds per square foot was assumed for the comparison presented herein.

As can be seen in figure 31, the minimum speed of each configuration shown was limited by factors other than maximum lift coefficient. The minimum speed of the fixed-canard arrangement was limited by the trim capability of the canard ($\text{at } 1.24\ V_{stall}$) and the minimum speed of the free-floating-canard arrangement was limited by zero directional stability ($\text{at } 1.18\ V_{stall},\ \delta_f = 0^\circ$; and $1.07\ V_{stall},\ \delta_f = 10^\circ$). In cases in which the landing attitude of an aircraft is limited to lower angles (because of ground clearance or flying on the backside of the power curve), the limits cited above would be unrealistic for the landing approach and touchdown; however, they would still apply in low-altitude pull-up maneuvers.

The curves on figure 31 show that the velocity of the free-floating canard arrangement with the flaps neutral was slightly higher for a given angle of attack than that with the canard fixed. With the flaps deflected 10°, the velocity of the free-floating canard arrangement for a given angle of attack was less than the fixed-canard arrangement with the flaps neutral. For example, at $\alpha = 14^\circ$ the velocity with the free-floating canard was about 137 knots as compared to 157 knots with the fixed canard.

SUMMARY OF RESULTS

The results of the investigation to determine the low-speed static longitudinal and lateral characteristics of a delta-wing canard model with the canard-surfaces fixed and free floating may be summarized as follows:

1. The trim lift capability of the free-floating-canard-surface arrangement was superior to that with the canard-surface fixed. The free-floating-canard-surface arrangement with twin vertical tails, the full-span flap deflected 10° and a static margin of 0.075 could be trimmed to a lift coefficient of 1.2 at an angle of attack of 27°. The 10° flap reduced the angle of attack for a given lift coefficient by about 5°.

2. The fixed-canard-surface arrangement with twin vertical tails and neutral flaps and having a static margin of 0.02 could be trimmed to a lift coefficient of 0.8 at an angle of attack of 18°.

3. The low speed trim capability of a composite-canard-surface arrangement for which the canard surface was fixed at supersonic speeds and free floating at subsonic speeds was generally comparable to that with the canard-surface fixed.

4. The model with the single center vertical tail was directionally unstable at lift coefficients above 0.8 whether the canard surface was fixed or free floating.

5. With a static margin of $0.02\bar{c}$, the model with twin vertical tails and having the canard-surface fixed was directionally stable to a trim lift coefficient of 0.82, the highest trim lift coefficient attainable.

6. The free-floating-canard-surface arrangement with twin vertical tails had less directional stability than the fixed-canard-surface arrangement because of the more rearward center-of-gravity location and the low canard-surface deflections required for trim. However, with the static margin increased from $0.01\bar{c}$ to $0.075\bar{c}$, the canard-surface-free-floating

model with flaps neutral was stable to a trim lift coefficient of 0.9, and with the flaps deflected 10°, the model was directionally stable to a trim lift coefficient of 1.2.

Langley Research Center,
National Aeronautics and Space Administration,
Langley Field, Va., July 15, 1959.

REFERENCES

1. Driver, Cornelius: Longitudinal and Lateral Stability and Control Characteristics of Two Canard Airplane Configurations at Mach Numbers of 1.41 and 2.01. NACA RM L56L19, 1957.

2. Spearman, M. Leroy, and Driver, Cornelius: Some Factors Affecting the Stability and Performance Characteristics of Canard Aircraft Configurations. NACA RM L58D16, 1958.

3. Mathews, Charles W.: Study of the Canard Configurations With Particular Reference to Transonic Flight Characteristics and Low-Speed Characteristics at High Lift. NACA RM L8G14, 1949.

4. Sleeman, William C., Jr.: Investigation at High Subsonic Speeds of the Static Longitudinal and Lateral Stability Characteristics of Two Canard Airplane Configurations. NACA RM L57J08, 1957.

5. Bates, William R.: Low-Speed Static Longitudinal Stability Characteristics of a Canard Model Having a 60° Triangular Wing and Horizontal Tail. NACA RM L9H17, 1949.

6. McLemore, H. Clyde: Low-Speed Investigation of the Effects of Wing Leading-Edge Modifications and Several Outboard Fin Arrangements on the Static Stability Characteristics of a Large-Scale Triangular Wing. NACA RM L51J05, 1952.

7. Jaquet, Byron M., and Brewer, Jack D.: Effects of Various Outboard and Central Fins on Low-Speed Static-Stability and Rolling Characteristics of a Triangular-Wing Model. NACA RM L9E18, 1949.

8. Mitchum, Grady L., Crabill, Norman L., and Stevens, Joseph E.: Flight Determination of the Drag and Longitudinal Stability and Control Characteristics of a Rocket-Powered Model of a 60° Delta-Wing Airplane From Mach Numbers of 0.75 to 1.70. NACA RM L51I04, 1951.

9. Bates, William R.: Low-Speed Static Lateral Stability Characteristics of a Canard Model Having a 60° Triangular Wing and Horizontal Tail. NACA RM L9J12, 1949.

10. Johnson, Joseph L., Jr.: A Study of the Flow Field Behind the Triangular Horizontal Tail of a Canard Airplane at Approximately the Vertical-Tail Location by Means of a Tuft Grid. NACA RM L52H11, 1952.

TABLE I.- MODEL CONFIGURATIONS AND RANGE OF TESTS

Designation	Configuration	β, deg	Flap	δ_f, deg	C_μ	Data presented in figures for -	
						Longitudinal	Lateral
$WFV_1H_2N_1$	Wing-body, center vertical tail, 0.15S fixed canard, nose upright	-5, 0	Neutral	0	0	5, 17	26
$WFV_1H_1N_1$	Wing-body, center vertical tail, 0.20S fixed canard, nose upright	-5, 0	Full span	0, 10	0	6, 7, 17, 18, 19, 20, 22	25
	Wing-body, center vertical tail, 0.20S free canard, nose upright	0	Full span	0, 10, 20	0	11, 13, 14, 15, 16, 20, 22	
			Inboard	35, 45	0.0052, 0.0074	12, 13	
$WFV_2H_1N_2$	Wing-body, outboard vertical tails, 0.20S fixed canard, nose inverted	-5, 0, 5	Full span	0, 10, 20	0	8, 9, 21, 31	28, 29, 30
WFV_1N_2	Wing-body, center vertical tail, nose inverted	-5, 0, 5	Neutral	0	0	10	23, 27, 28
WFV_2N_2	Wing-body, outboard vertical tails, nose inverted	0, 5	Neutral	0	0	10	28
WFV_1N_1	Wing-body, center vertical tail, nose upright	-5, 0	Neutral	0	0	11	23, 24, 25, 26
WFN_2	Wing-body, nose inverted	-10, 0, 5	Neutral	0	0		27
WFH_1N_2	Wing-body, 0.20S fixed canard, nose inverted	-5, 0, 5	Neutral	0	0		27
$WFV_1H_1N_2$	Wing-body, center vertical tail, 0.20S fixed canard, nose inverted	0, 5	Neutral	0	0		27, 28
$WFV_1N_1s_1$	Wing-body, center vertical tail, nose upright, strake 1	-5, 0	Neutral	0	0		24
$WFV_1H_1N_1s_2$	Wing-body, center vertical tail, 0.20S fixed canard, nose upright, strake 2	-5, 0	Neutral	0	0		25
$WFV_1H_2N_1s_2$	Wing-body, center vertical tail, 0.15S fixed canard, nose upright, strake 2	-5, 0	Neutral	0	0		26

Figure 1.- System of axes used. Arrows indicate positive direction of forces, moments, and angular displacements.

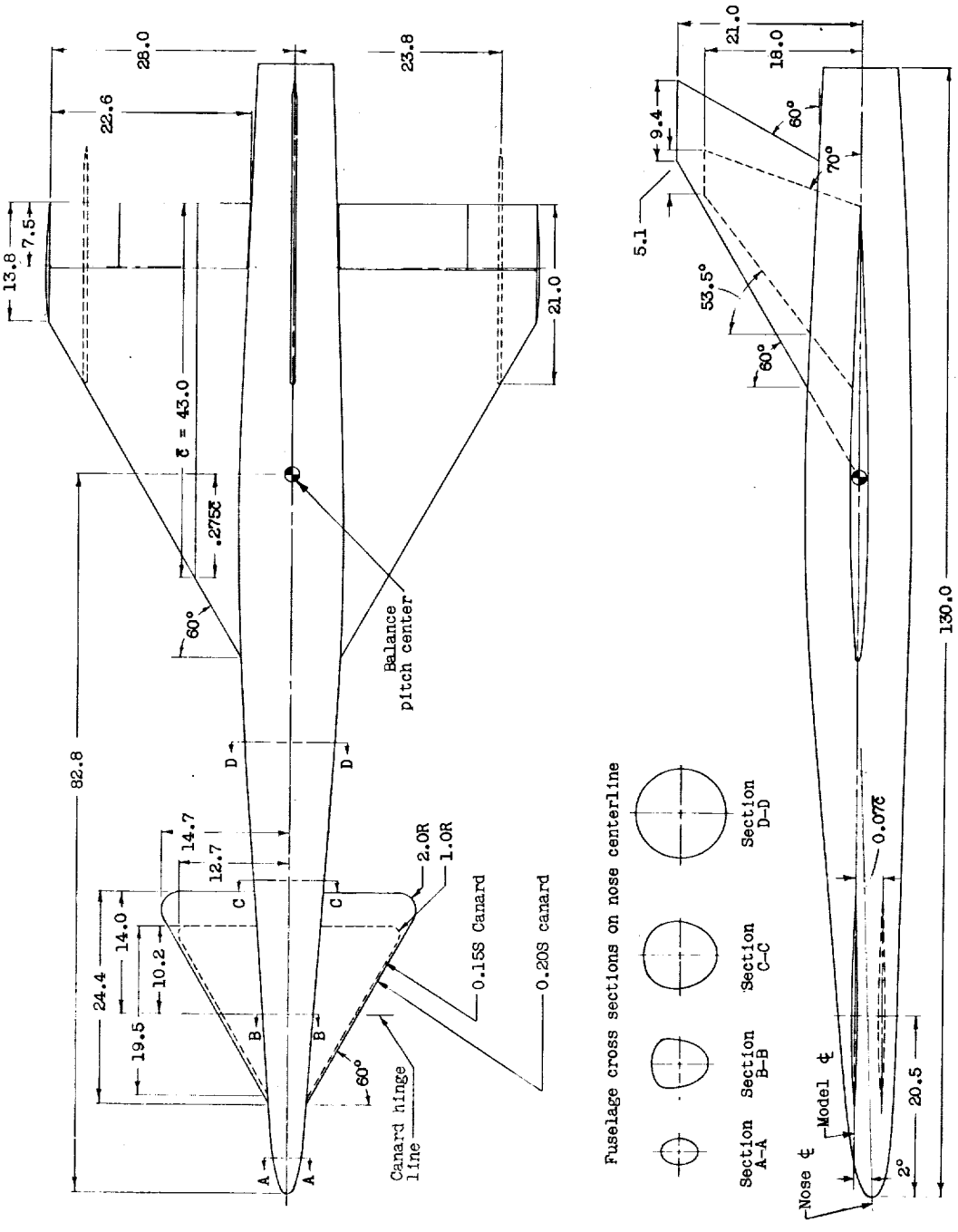

Figure 2.- General arrangement and principal dimensions of the model. (Dimensions are in inches.)

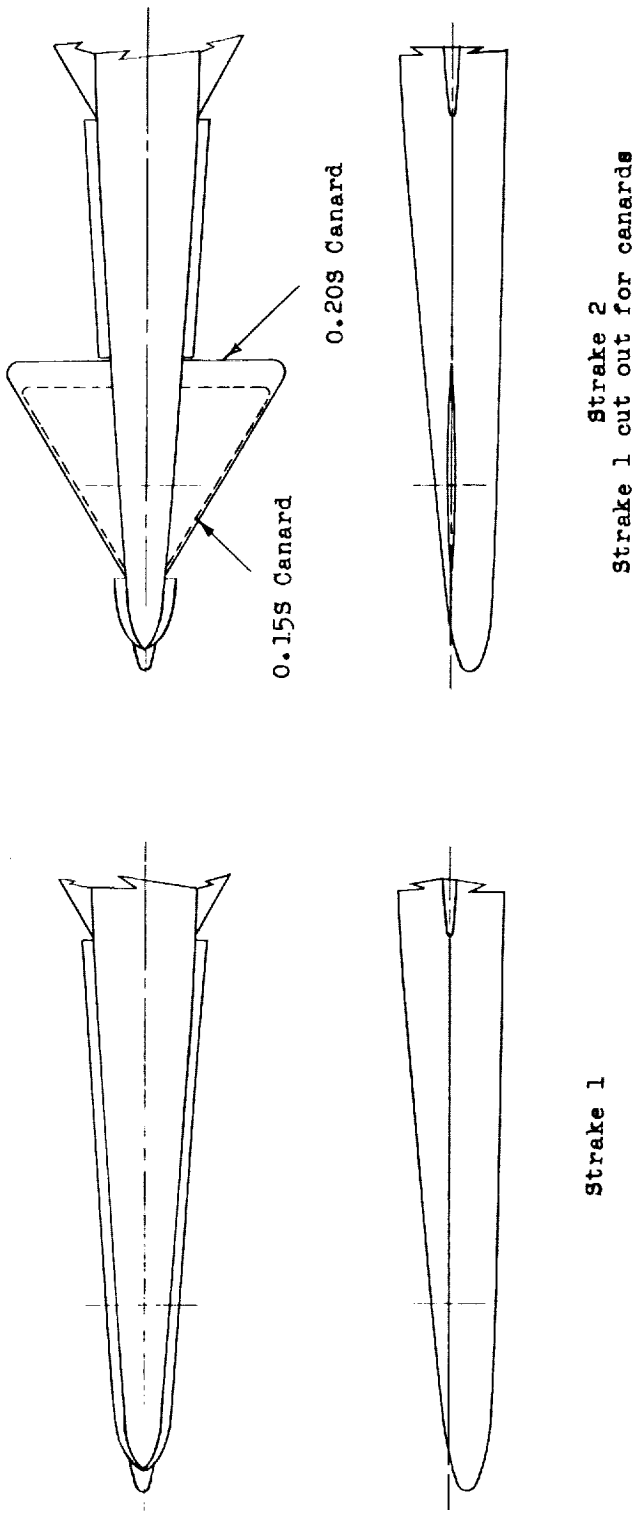

Figure 3.- Sketches of the nose strake.

L-57-1934

Figure 4.- Photograph of the delta-wing model in the Langley full-scale tunnel.

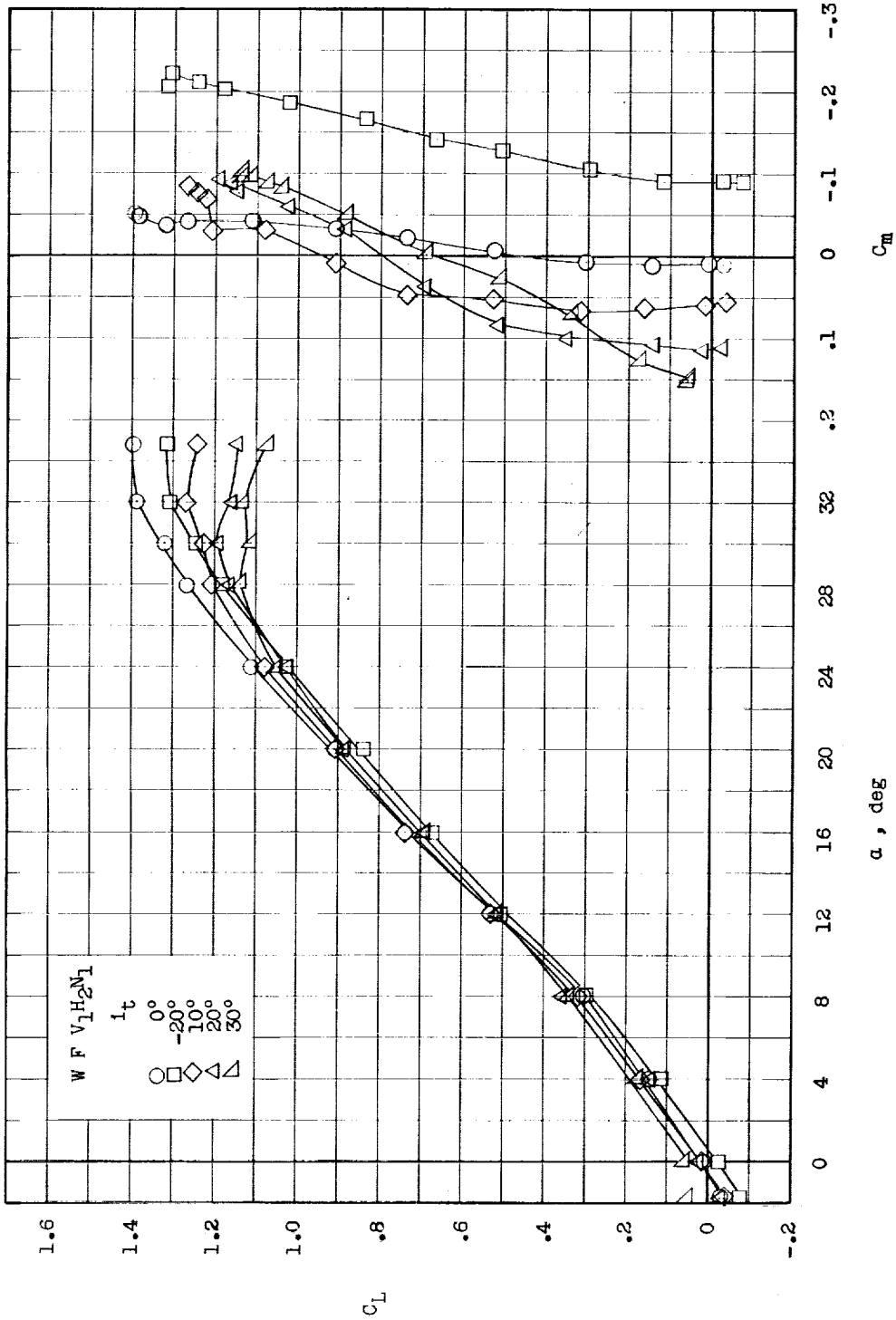

(a) Lift and pitching moment.

Figure 5.- Longitudinal characteristics of the model with a center vertical tail, nose upright, and a 0.15S fixed canard at several canard incidences. $\delta_f = 0^o$; center of gravity at 0.11$\bar{c}$.

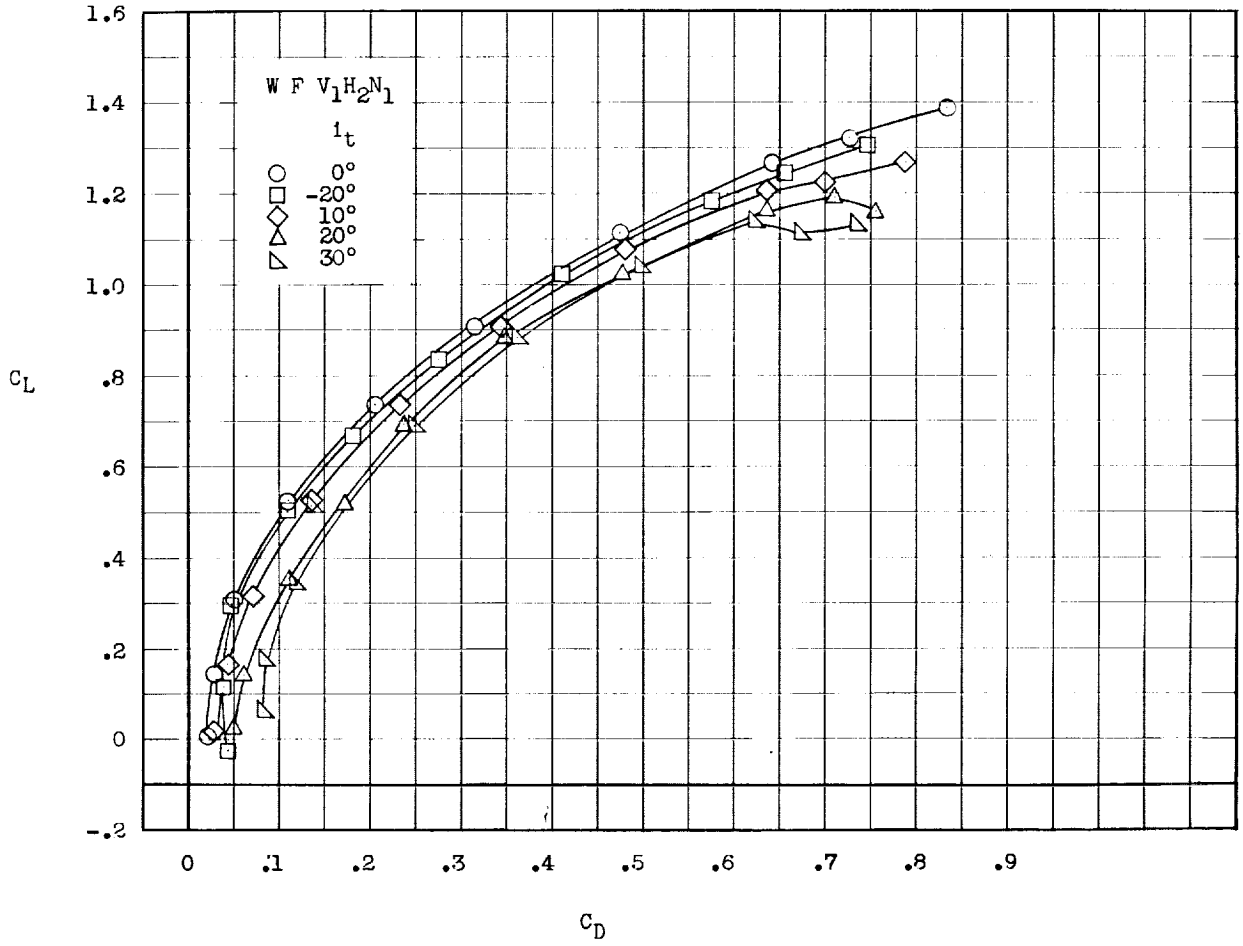

(b) Drag.

Figure 5.- Concluded.

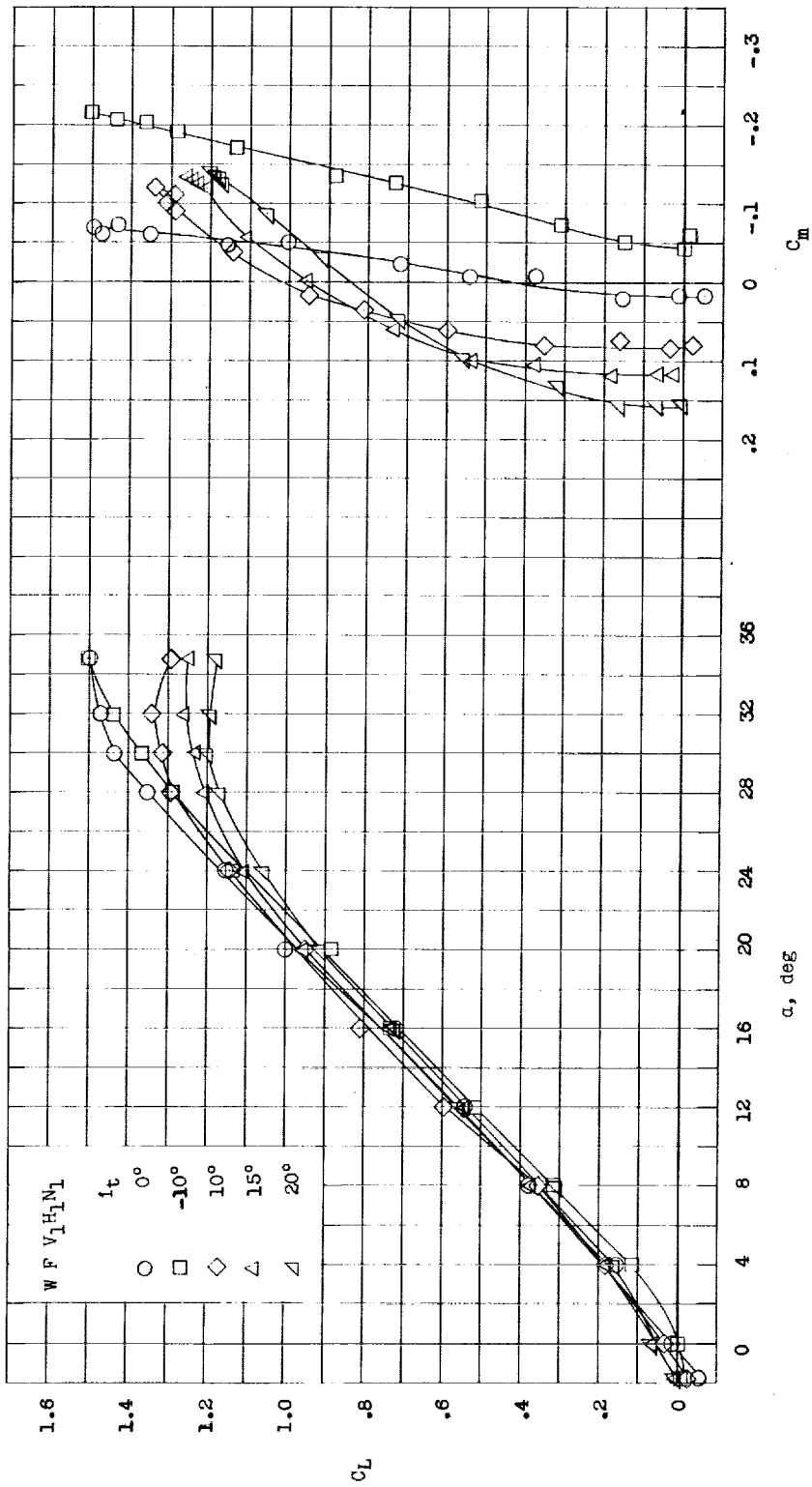

(a) Lift and pitching moment.

Figure 6.- Longitudinal characteristics of the model with a center vertical tail, nose upright, and a 0.20S fixed canard at several canard incidences. $\delta_f = 0°$; center of gravity at 0.025$\bar{c}$.

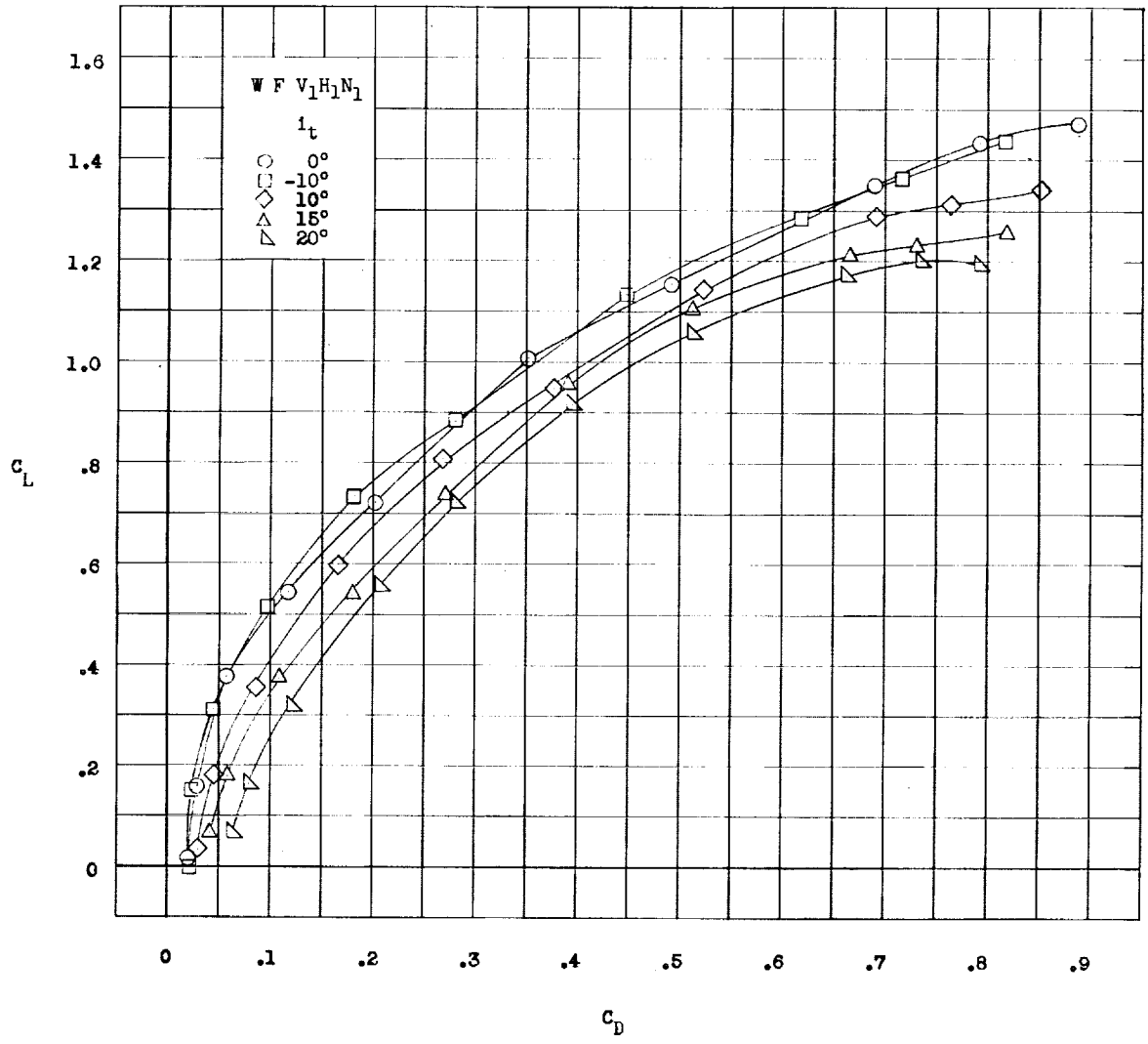

(b) Drag.

Figure 6.- Concluded.

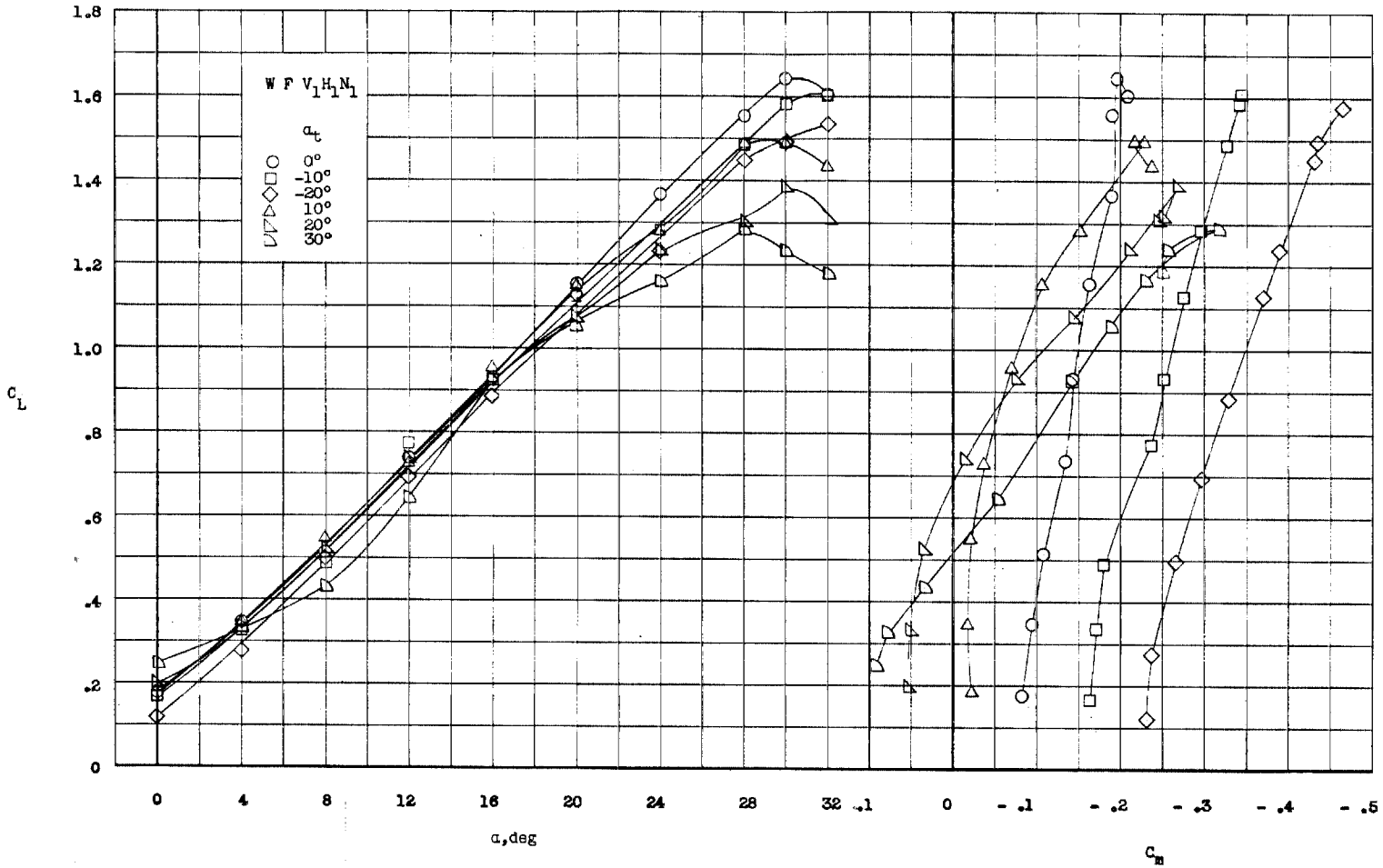

(a) Lift and pitching moment.

Figure 7.- Longitudinal characteristics of the model with a center vertical tail, nose inverted, a 0.20S fixed canard, and the full-span flaps deflected 10°. Center of gravity at 0.025$\bar{c}$.

CONFIDENTIAL

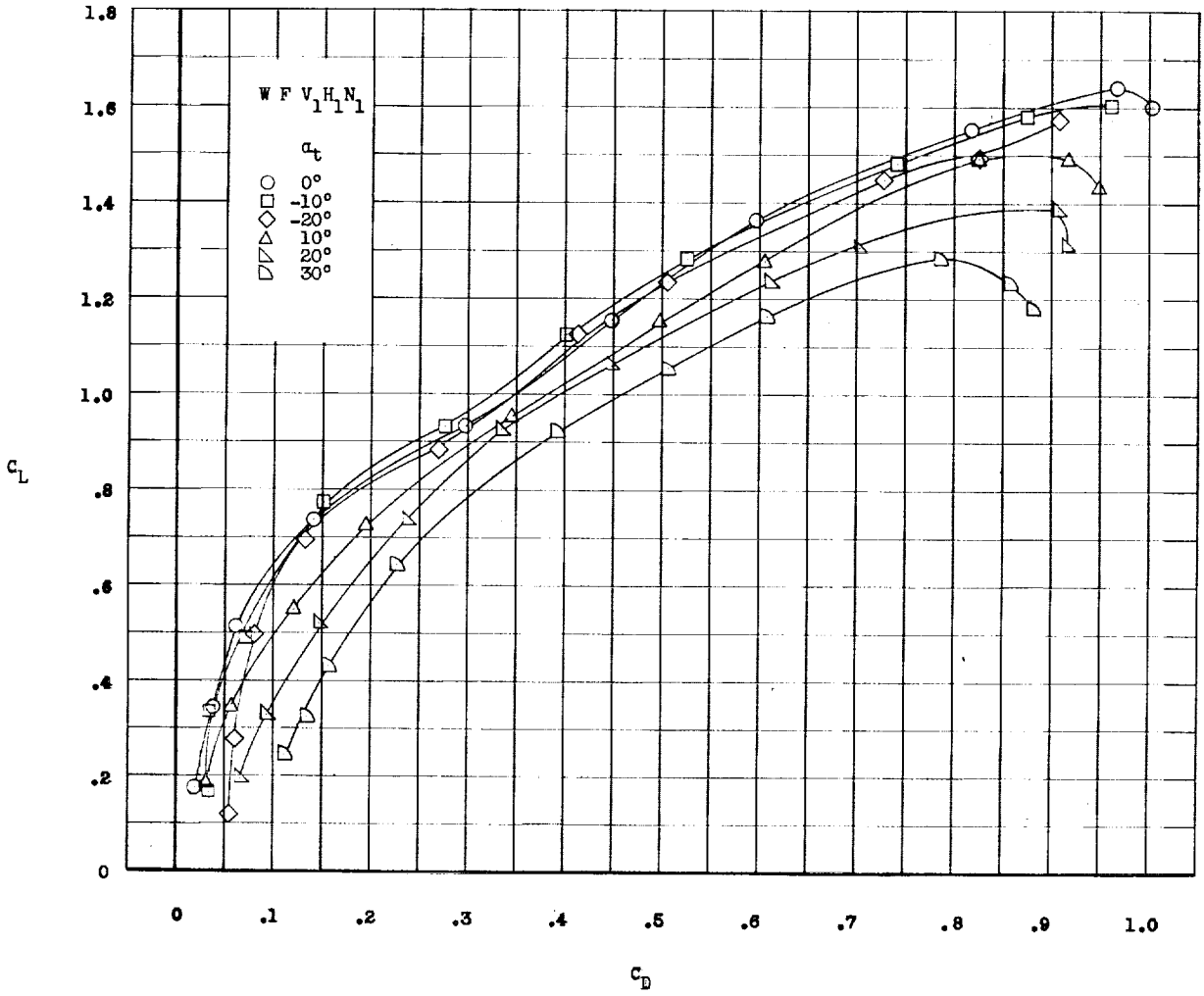

(b) Drag.

Figure 7.- Concluded.

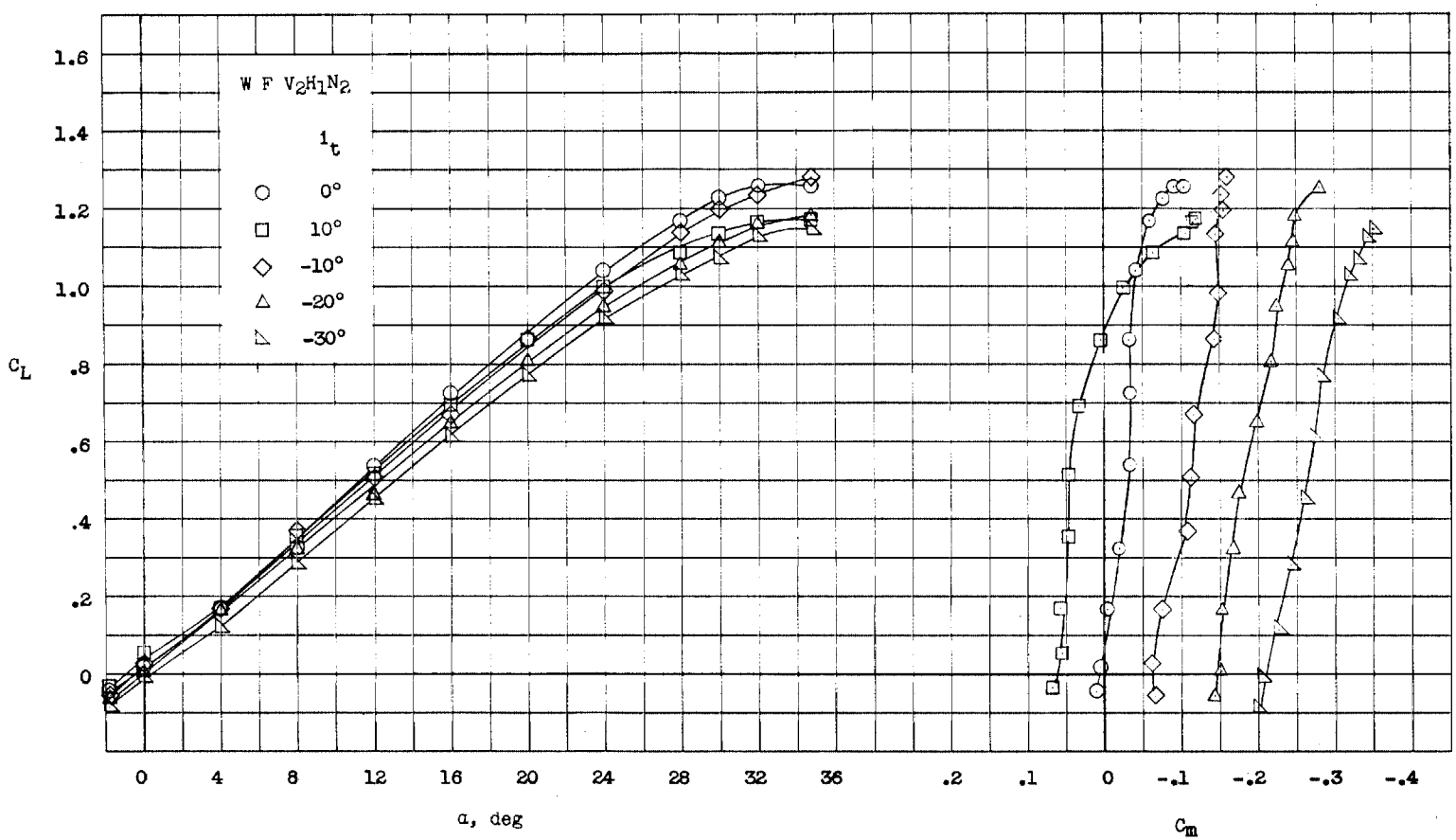

(a) Lift and pitching moment.

Figure 8.- Longitudinal characteristics of the model with twin vertical tails, nose inverted, and a 0.20S fixed canard at several canard incidences. $\delta_f = 0^\circ$; center of gravity at $-0.015\bar{c}$.

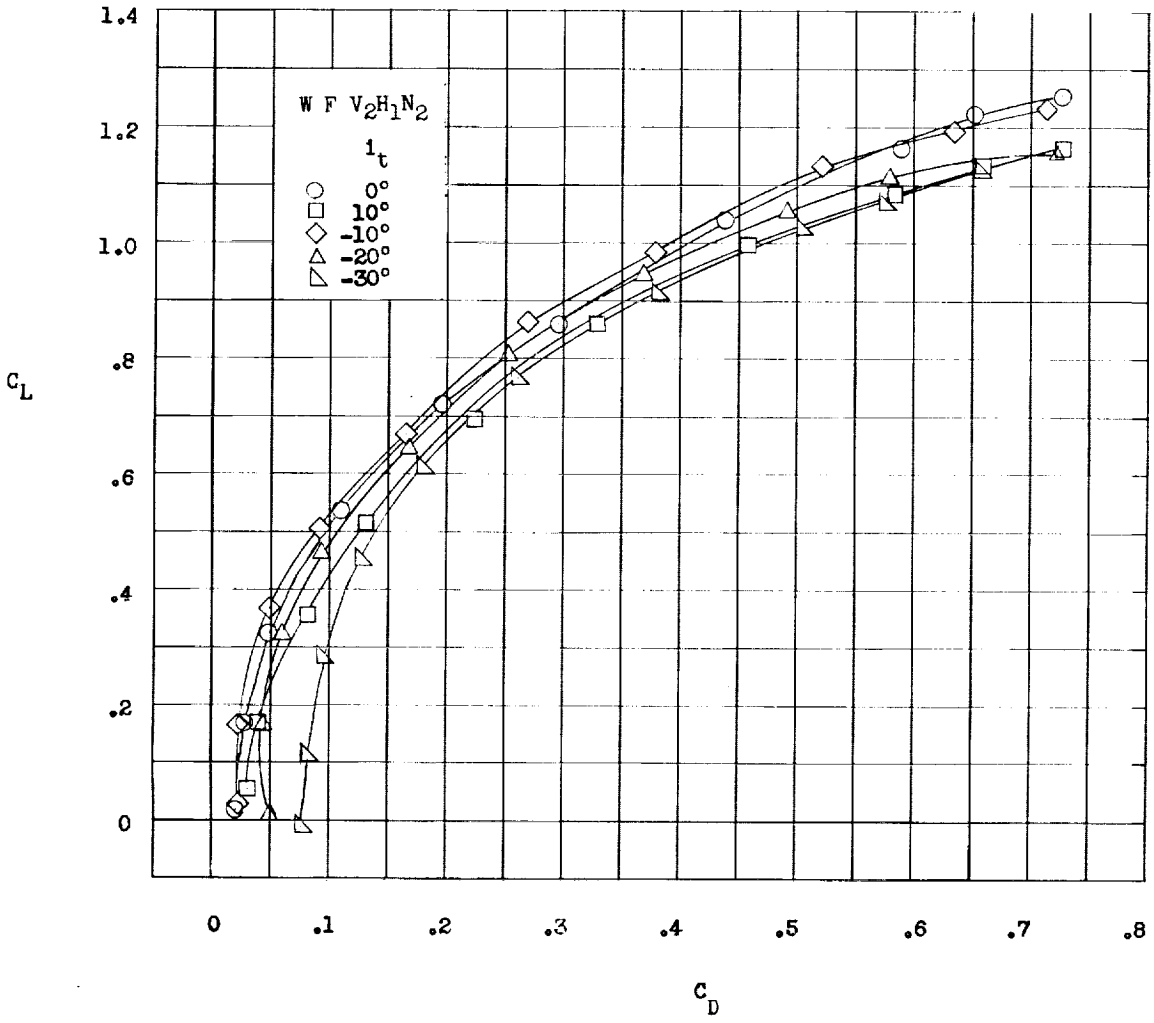

(b) Drag.

Figure 8.- Concluded.

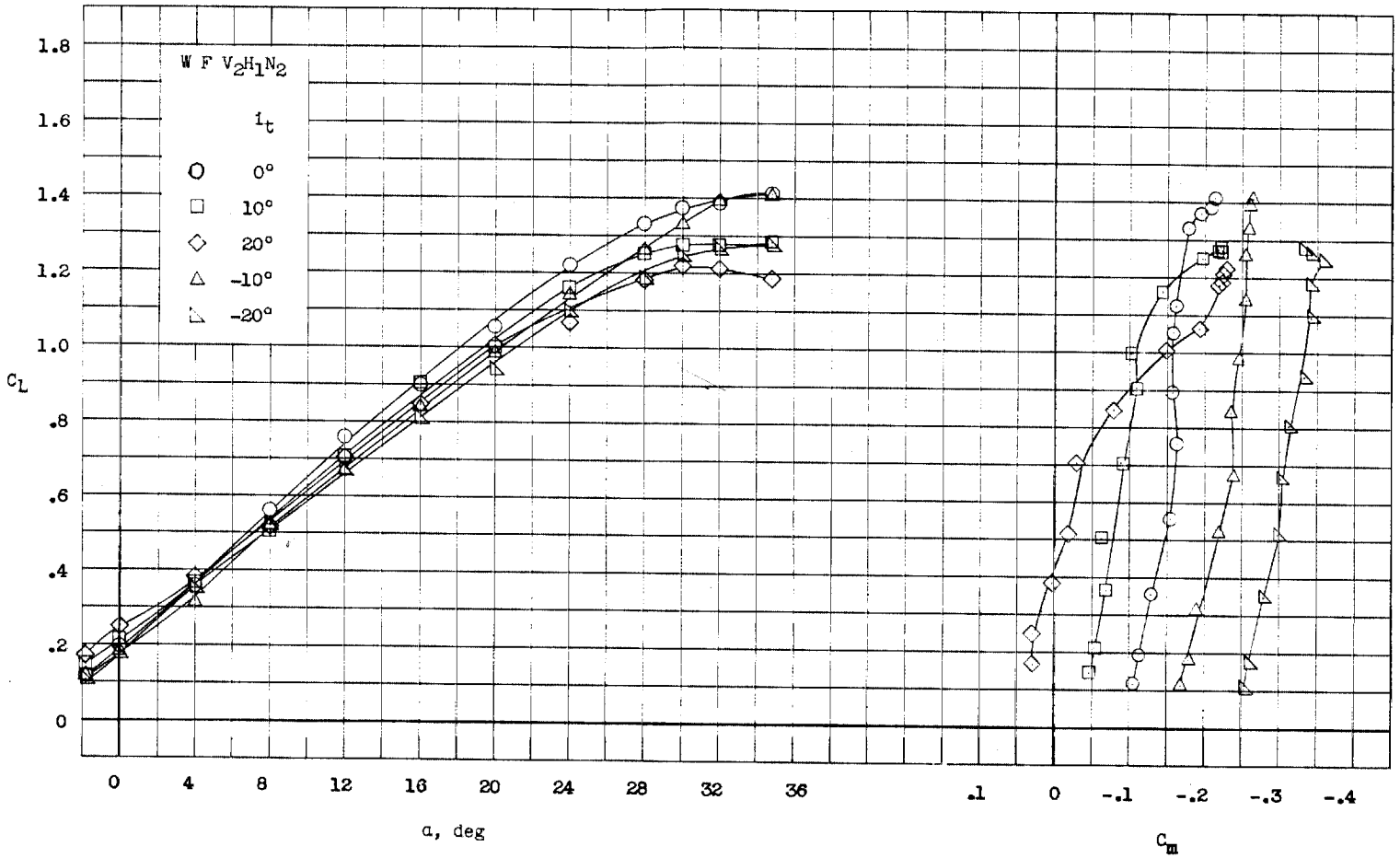

(a) Lift and pitching moment.

Figure 9.- Longitudinal characteristics of the model with twin vertical tails, nose inverted, and a 0.20S fixed canard at several canard incidences. $\delta_f = 10^o$; center of gravity at -0.015$\bar{c}$.

CONFIDENTIAL

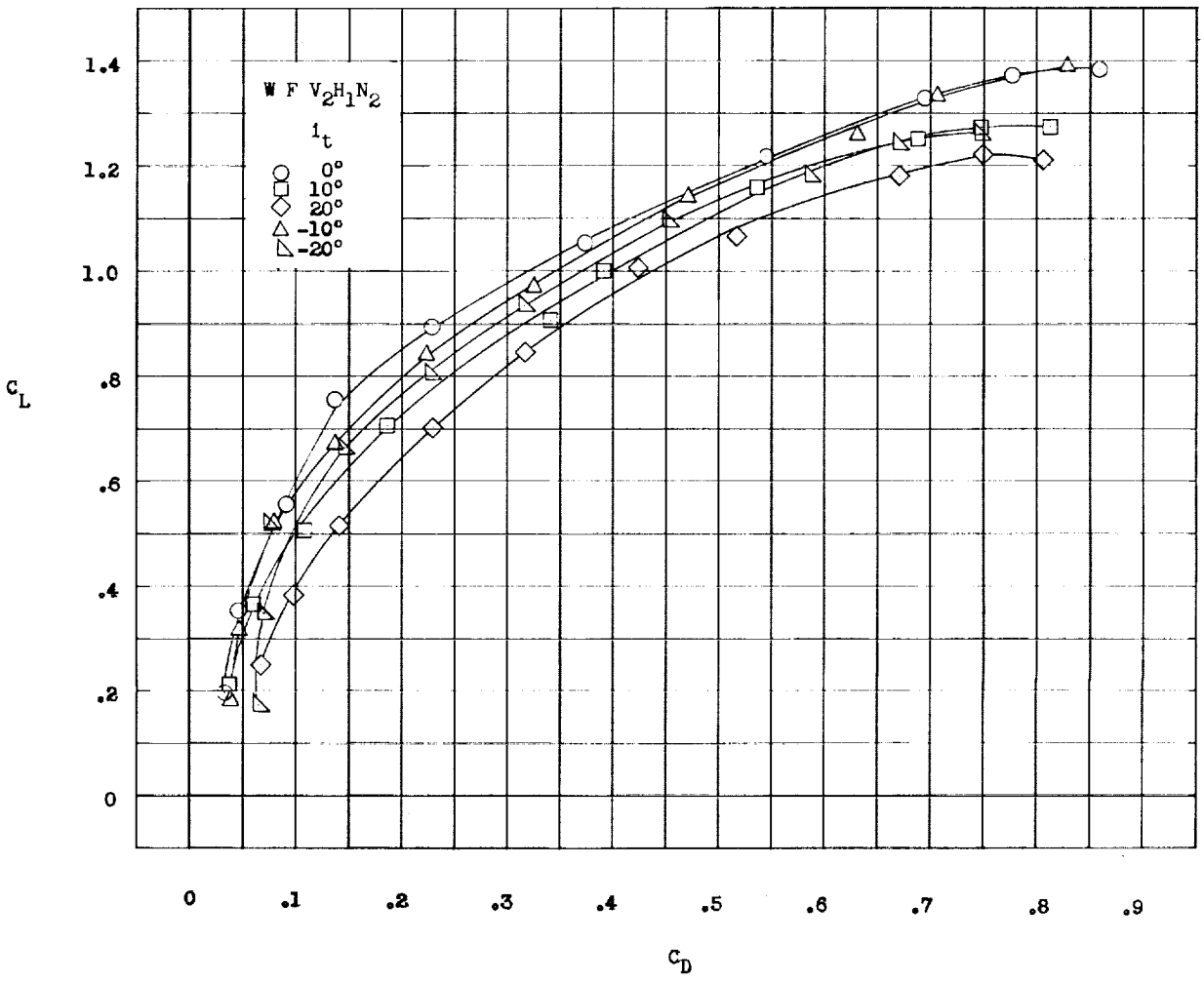

(b) Drag.

Figure 9.- Concluded.

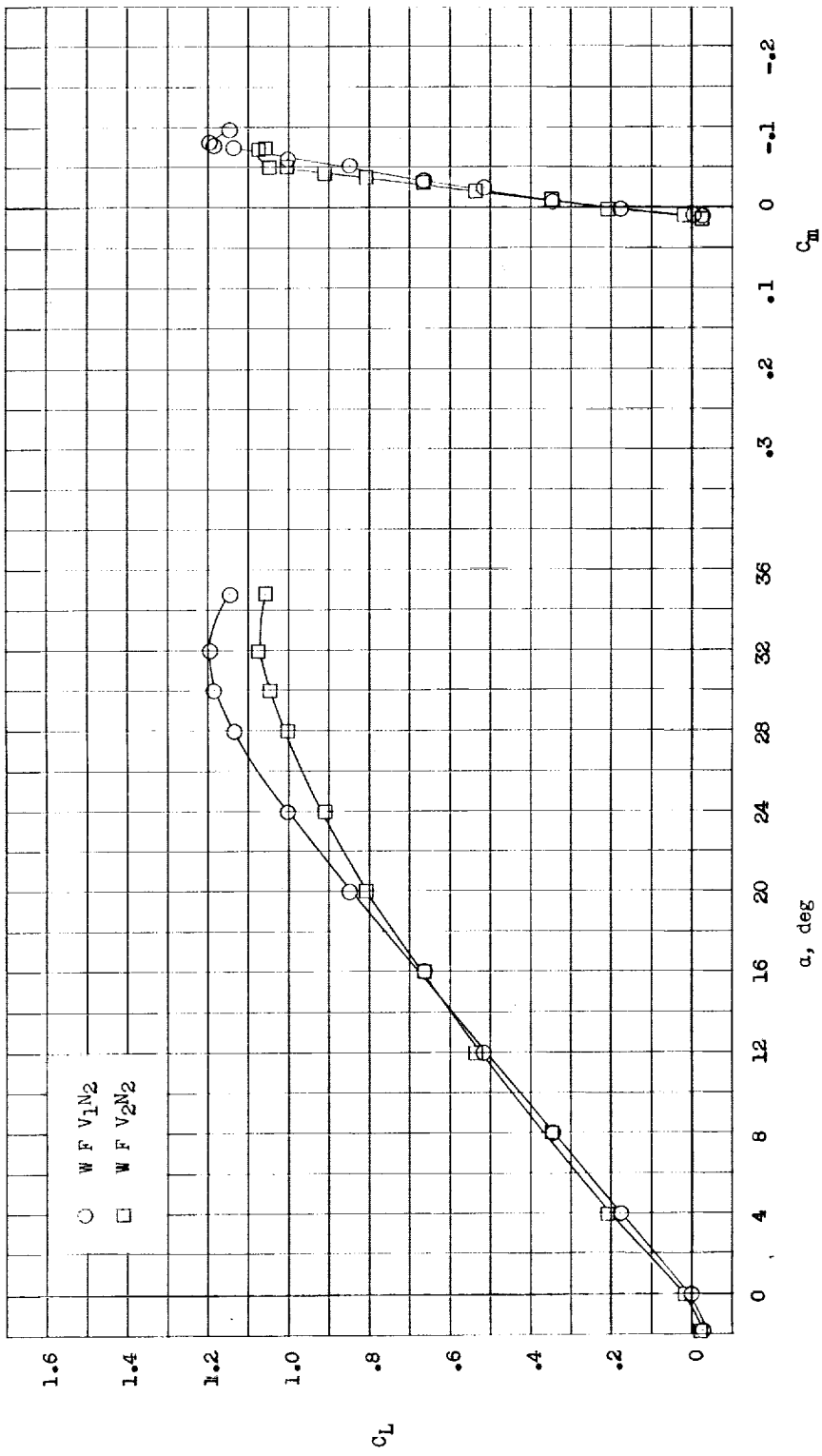

Figure 10.- Comparison of the longitudinal characteristics of the model with the single and twin vertical tails and nose inverted. $\delta_f = 0°$; center of gravity at 0.275$\bar{c}$.

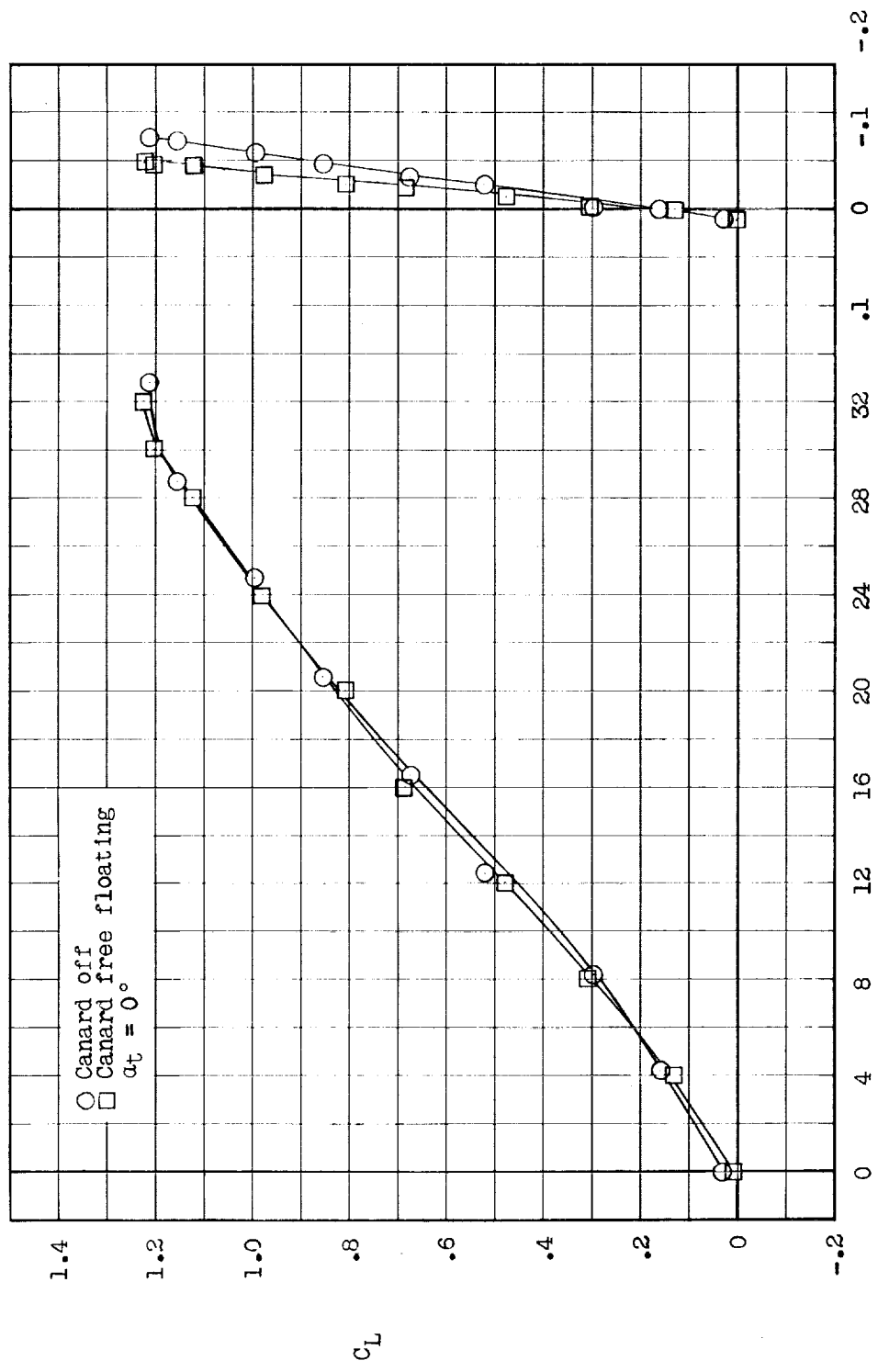

Figure 11.- Effect of the 0.20S free-floating canard on the longitudinal characteristics of the model with the center vertical tail and the nose upright. $\delta_f = 0°$; center of gravity at 0.27$\bar{c}$.

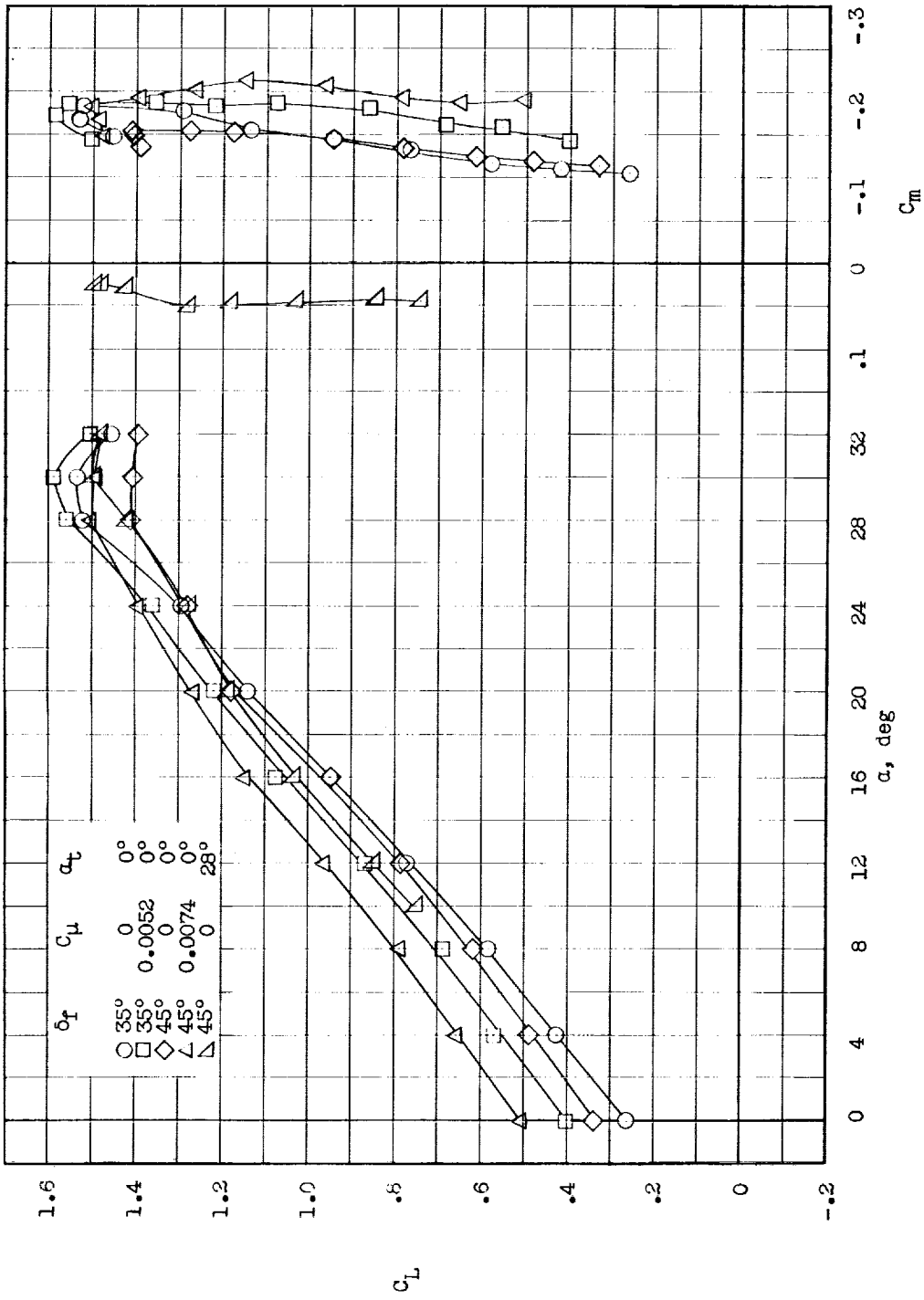

Figure 12.- Longitudinal characteristics of the model with a center vertical tail, nose upright, and a free-floating 0.20S canard and with the inboard flap deflected with and without blowing. Center of gravity at 0.27$\bar{c}$.

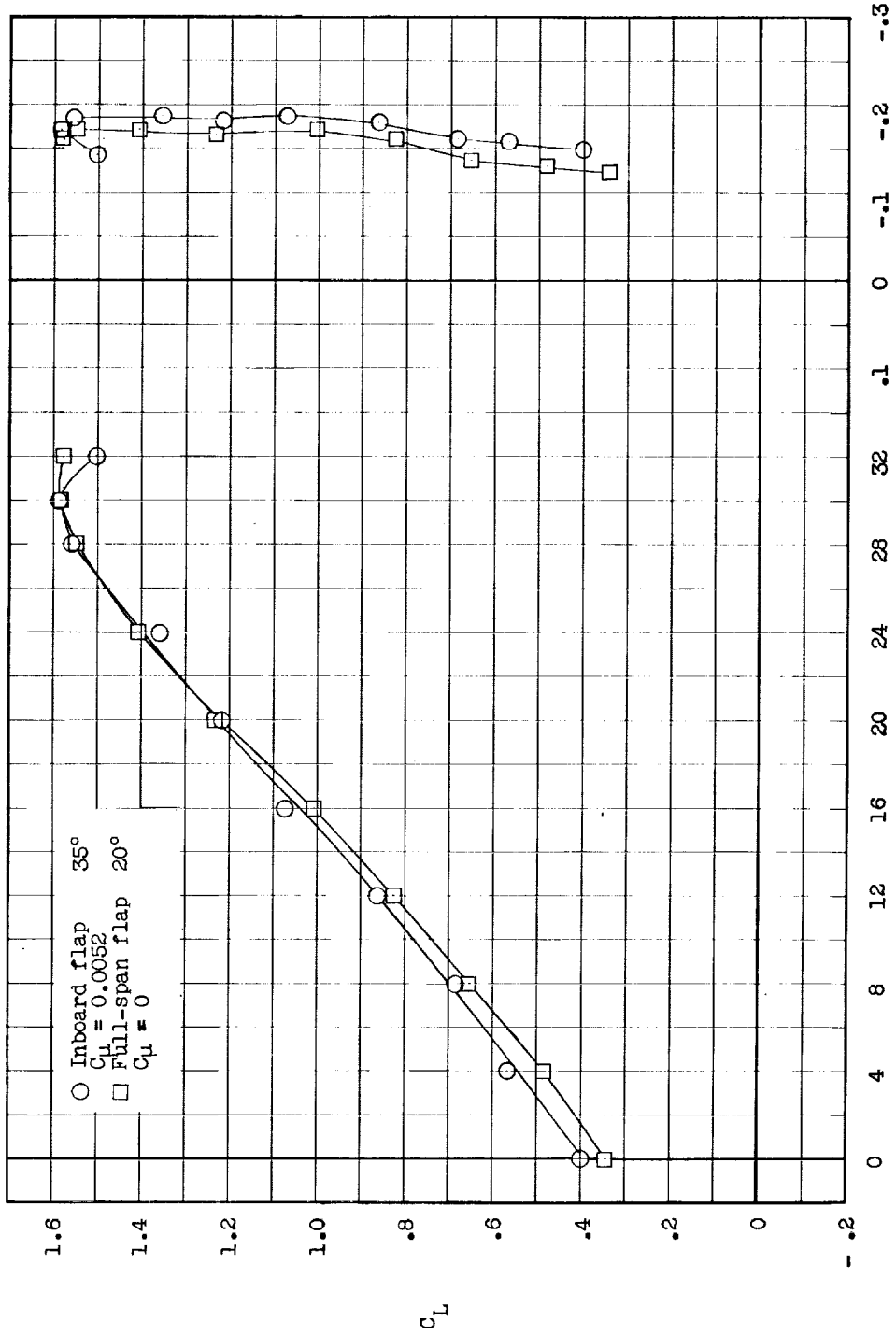

Figure 13.- Comparison of the longitudinal characteristics of the model with a center vertical tail, nose upright, and a free-floating canard for two wing-flap arrangements. Center of gravity at 0.275$\bar{c}$.

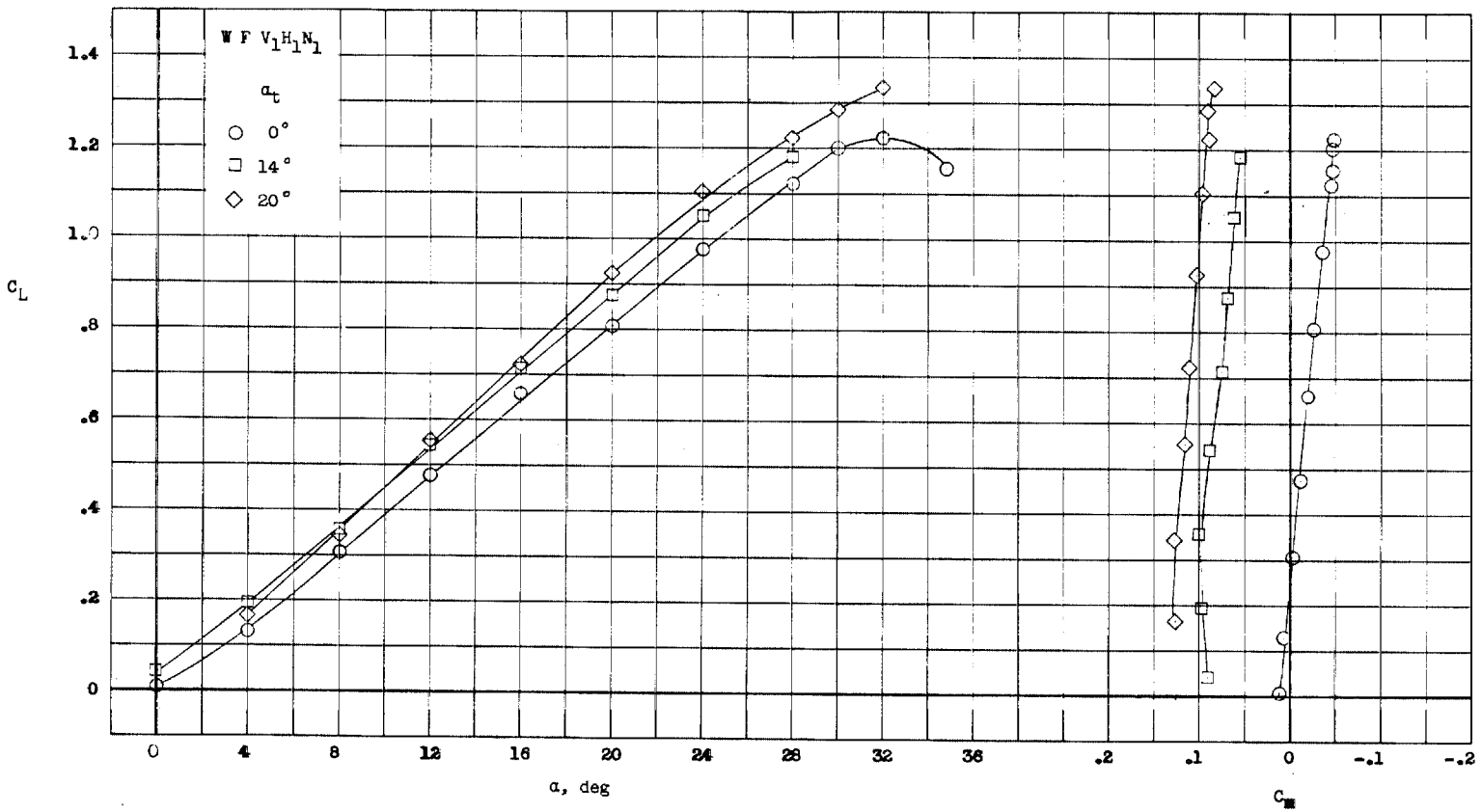

(a) Lift and pitching moment.

Figure 14.- Longitudinal characteristics of the model with a center vertical tail, nose upright, and a 0.20S free-floating canard at several canard-floating angles. $\delta_f = 0^o$; center of gravity at 0.275$\bar{c}$.

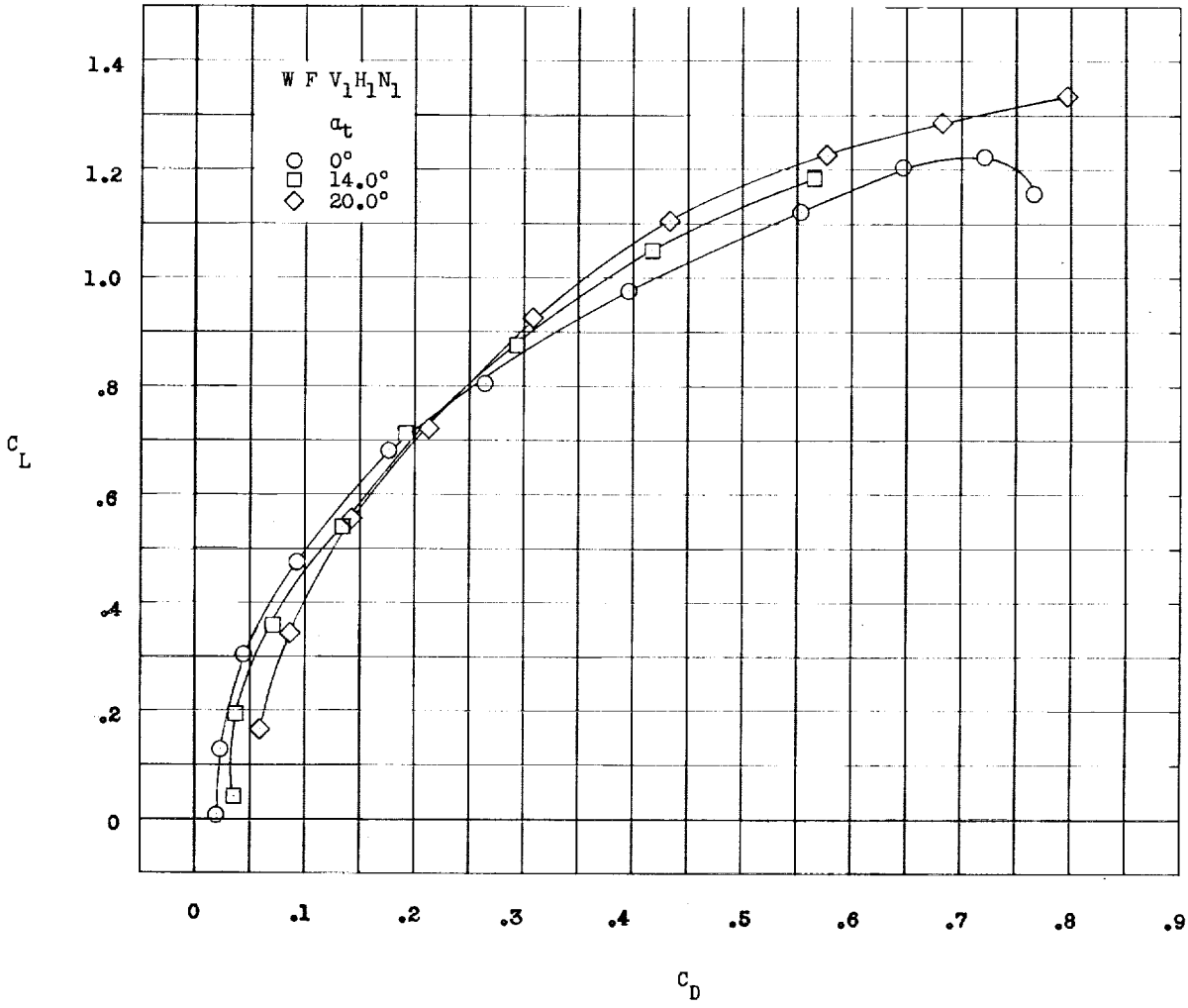

(b) Drag.

Figure 14.- Concluded.

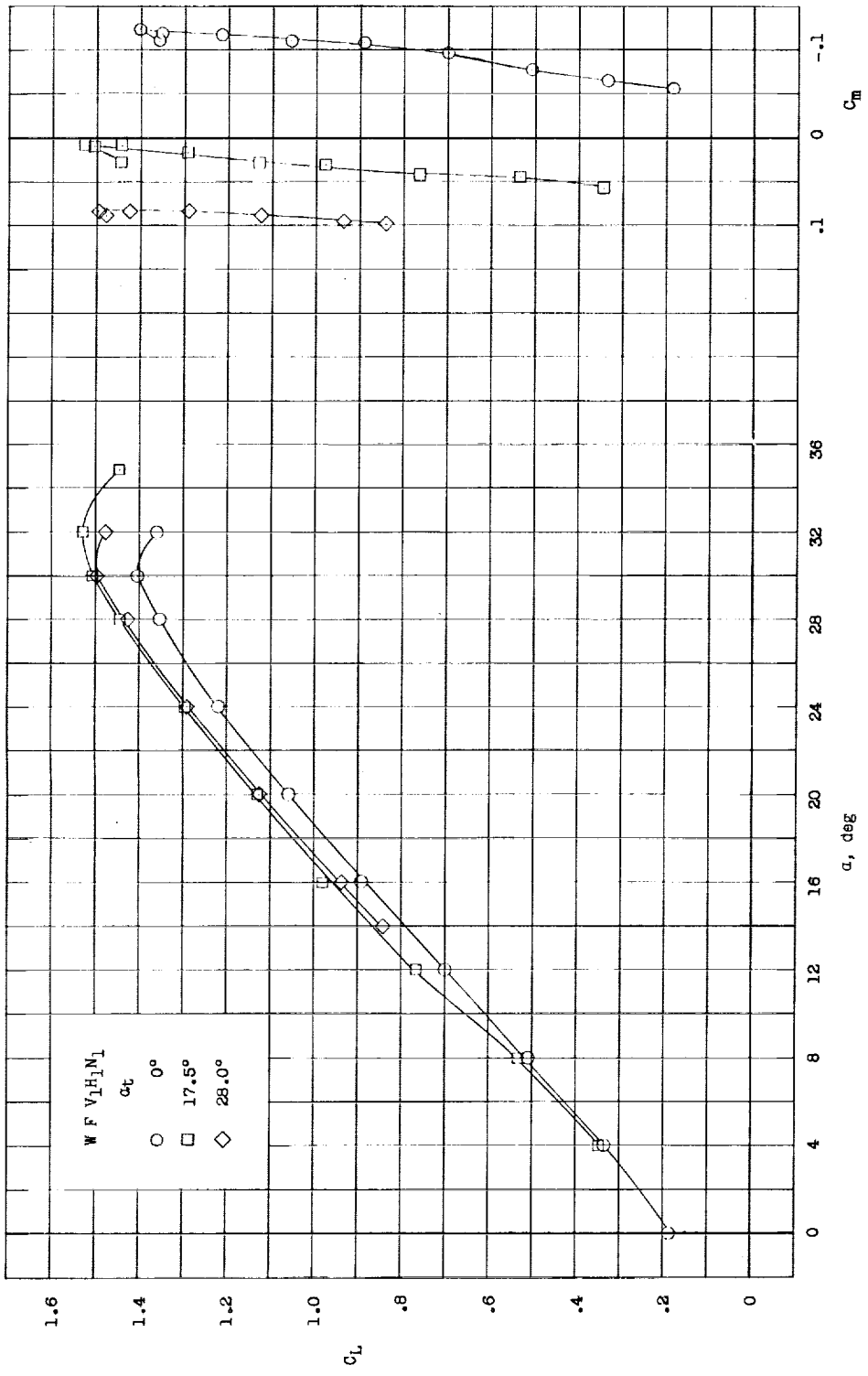

(a) Lift and pitching moment.

Figure 15.- Longitudinal characteristics of the model with a center vertical tail, nose upright, and a 0.20S free-floating canard at several canard-floating angles. Full-span flaps deflected 10°; center of gravity at 0.275c.

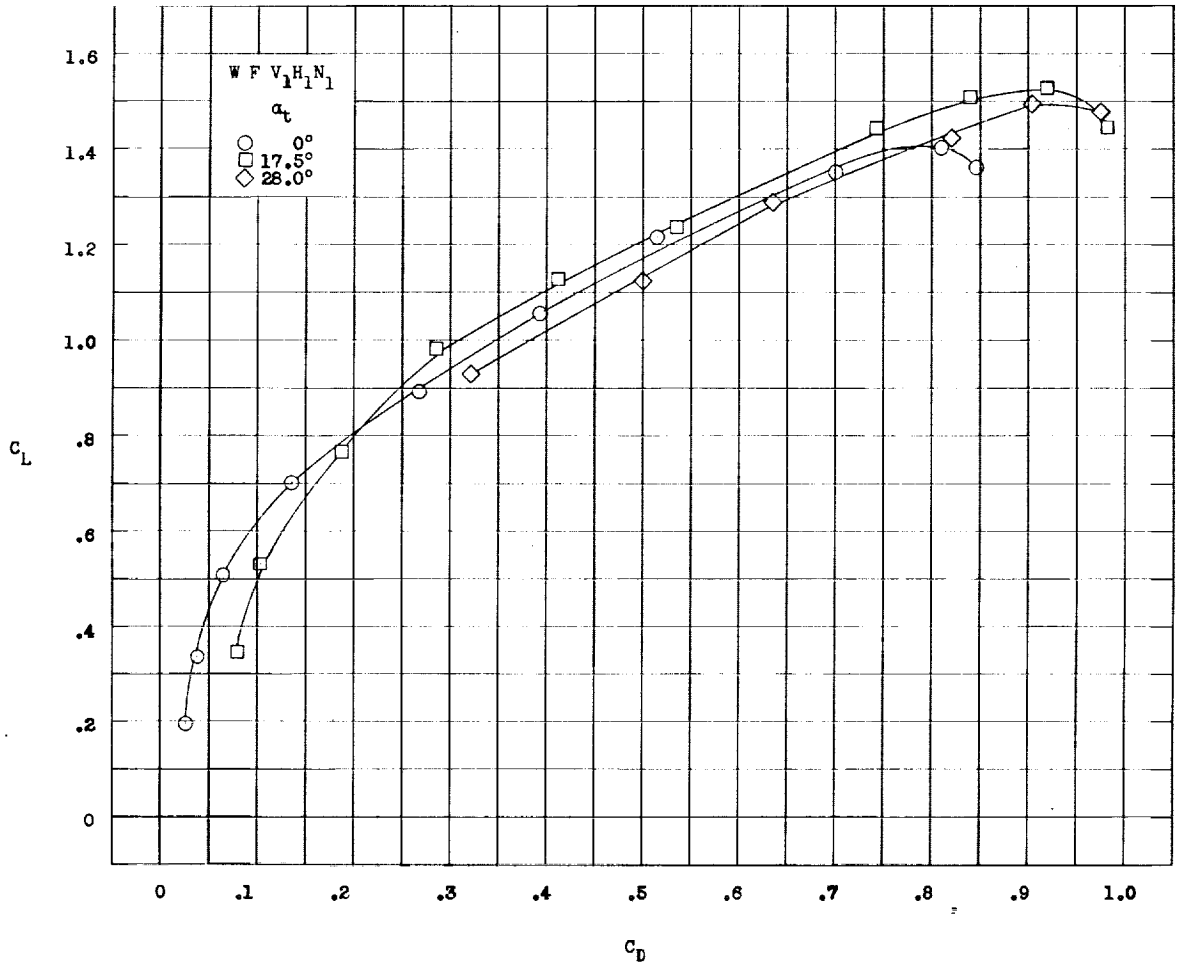

(b) Drag.

Figure 15.- Concluded.

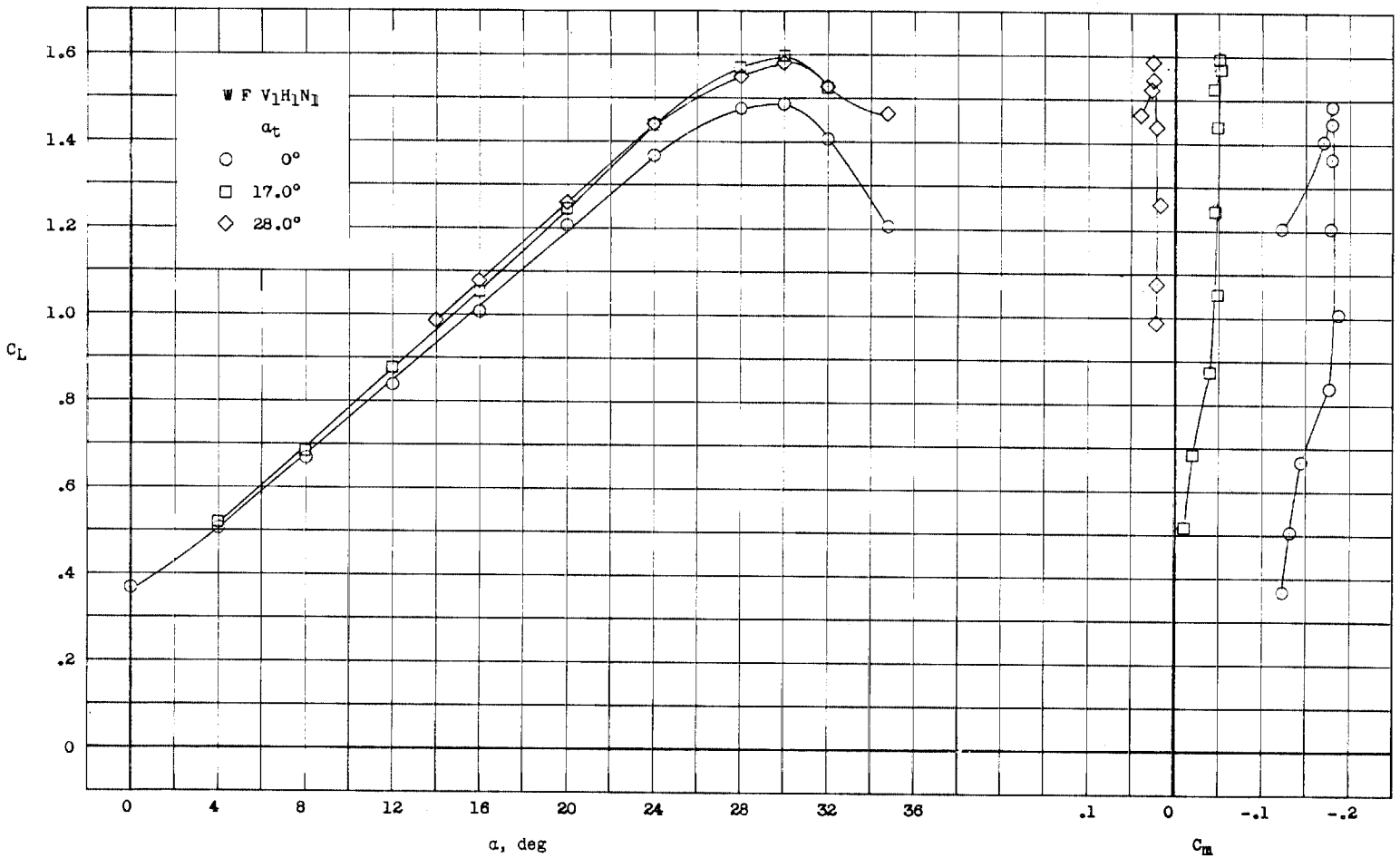

(a) Lift and pitching moment.

Figure 16.- Longitudinal characteristics of the model with a 0.20S free-floating canard at several canard-floating angles. Full-span flaps deflected 20°; center of gravity at 0.275$\bar{c}$.

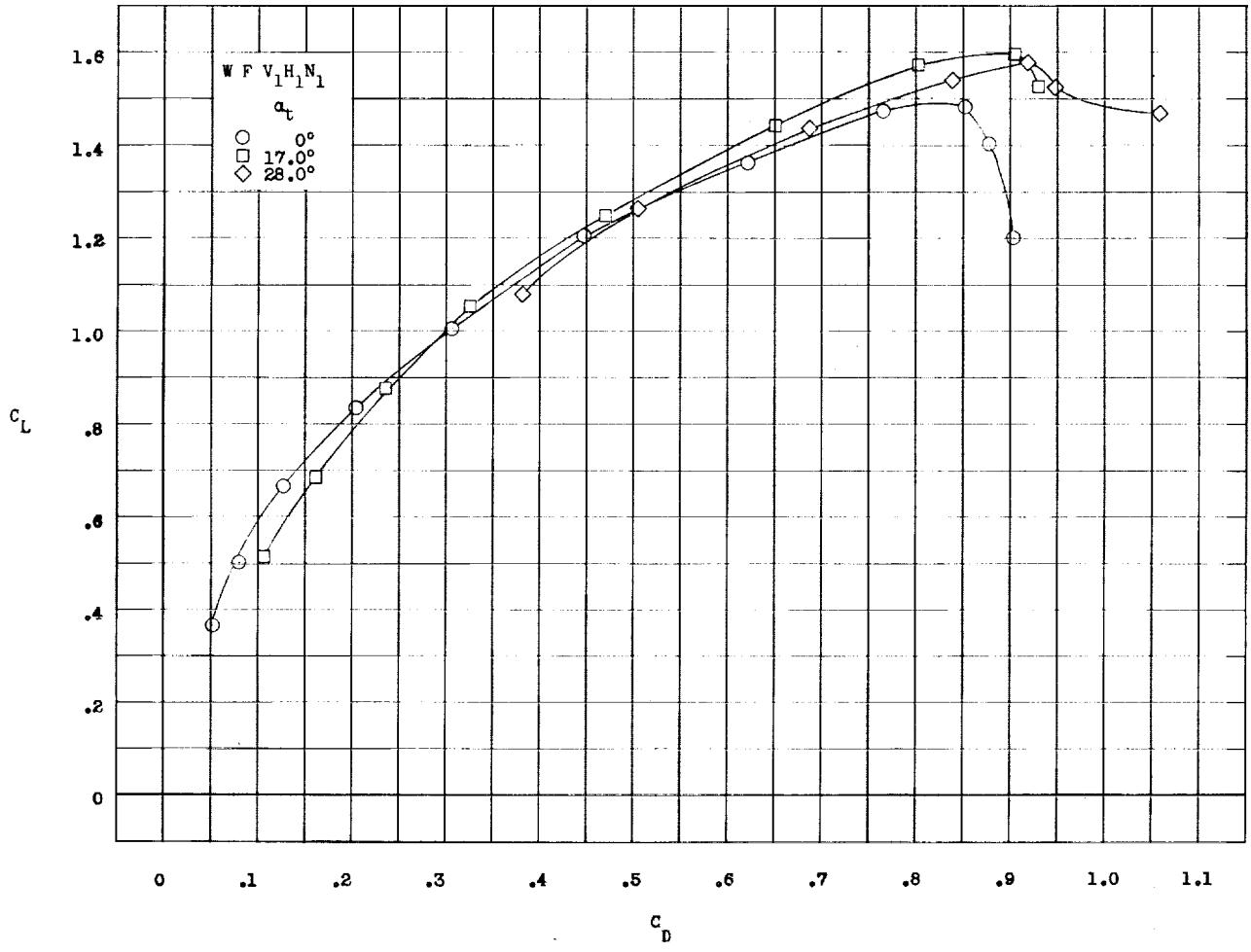

(b) Drag.

Figure 16.- Concluded.

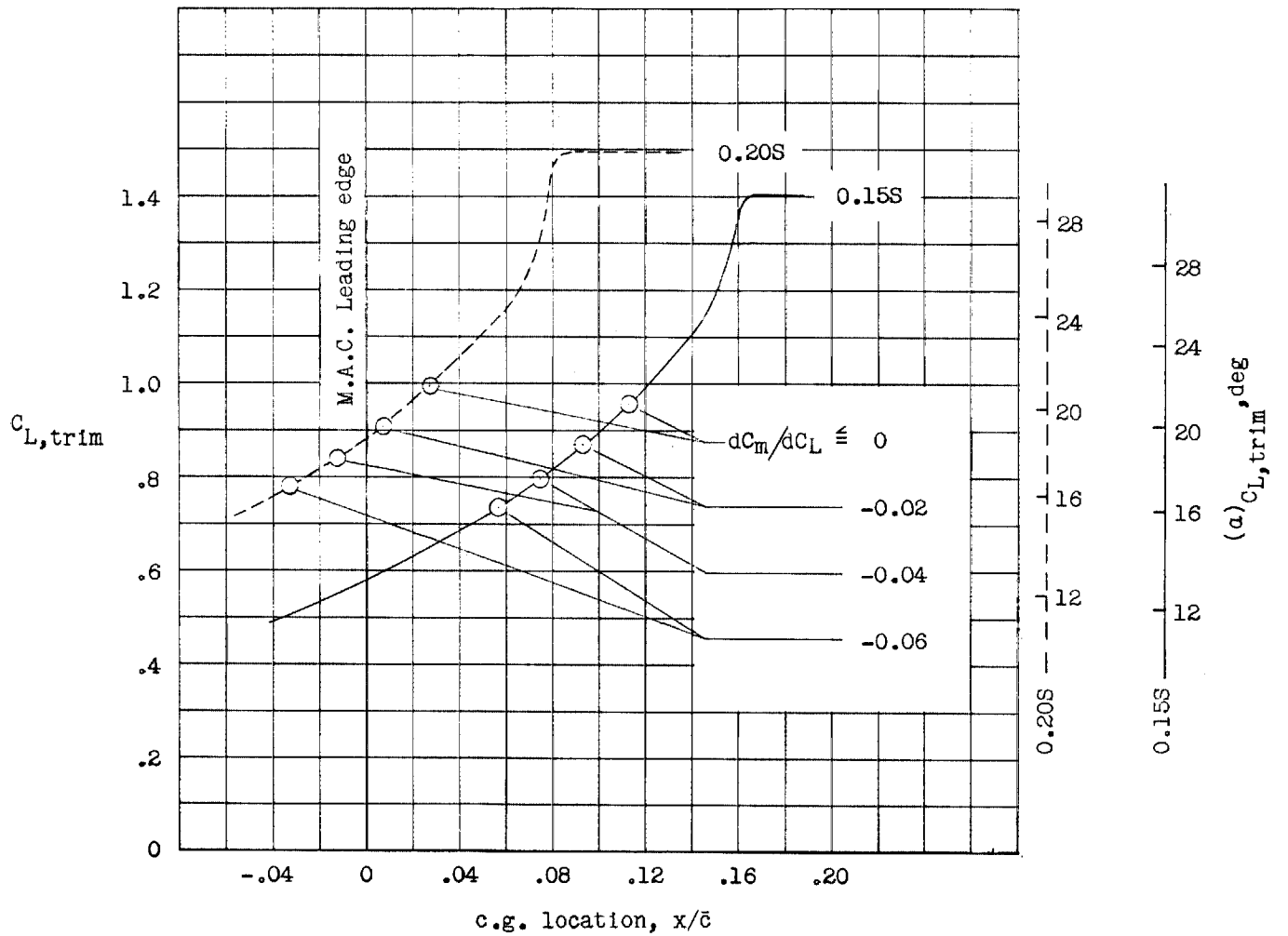

Figure 17.- Variation of maximum trim lift coefficient with center-of-gravity location of the model with an upright nose, center vertical tail, and the 0.15S and 0.20S fixed canards. $\delta_f = 0^o$.

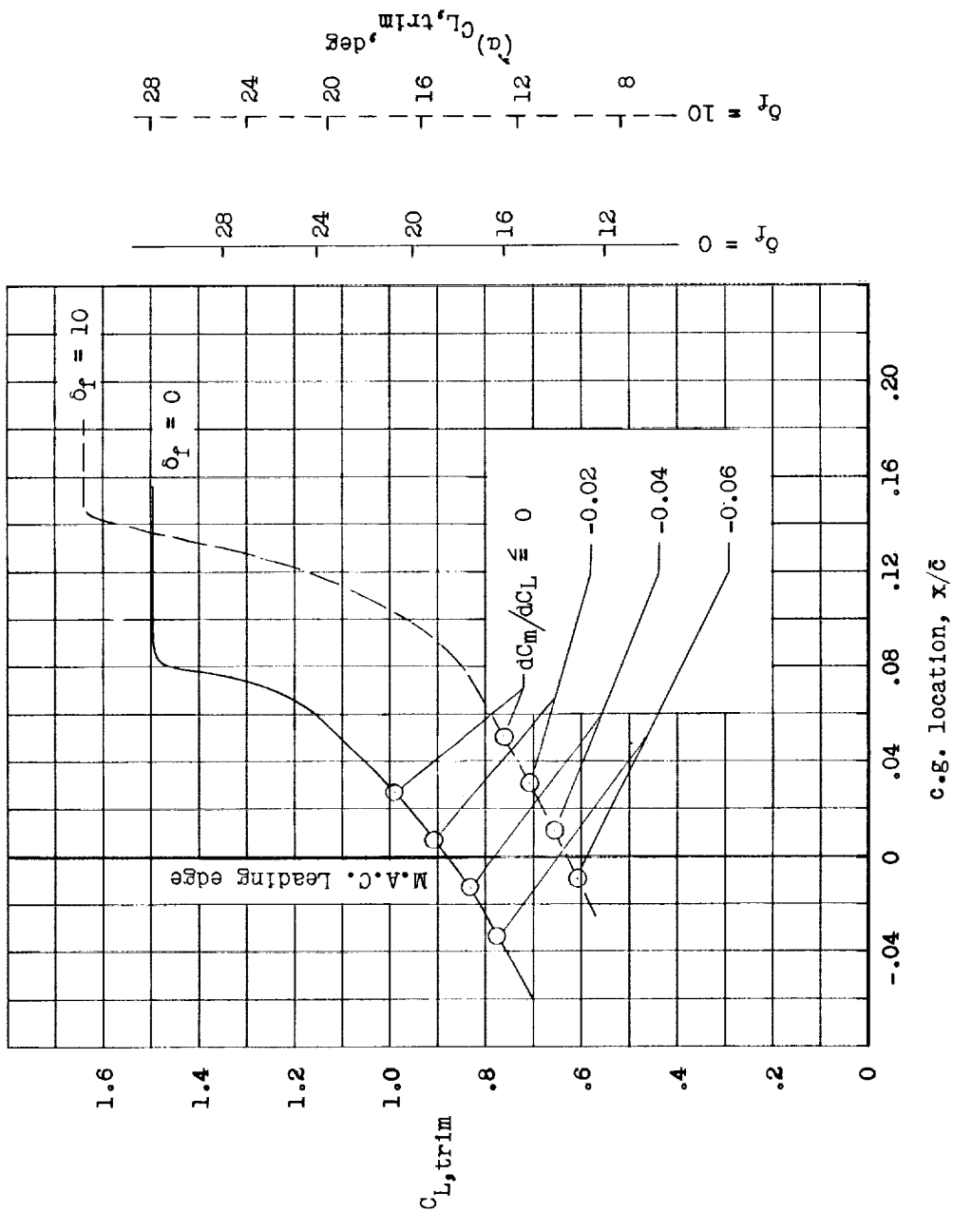

Figure 18.- Variation of maximum trim lift coefficient with center-of-gravity location of the model with an upright nose, center vertical tail, and a 0.20S fixed canard at two wing flap deflections.

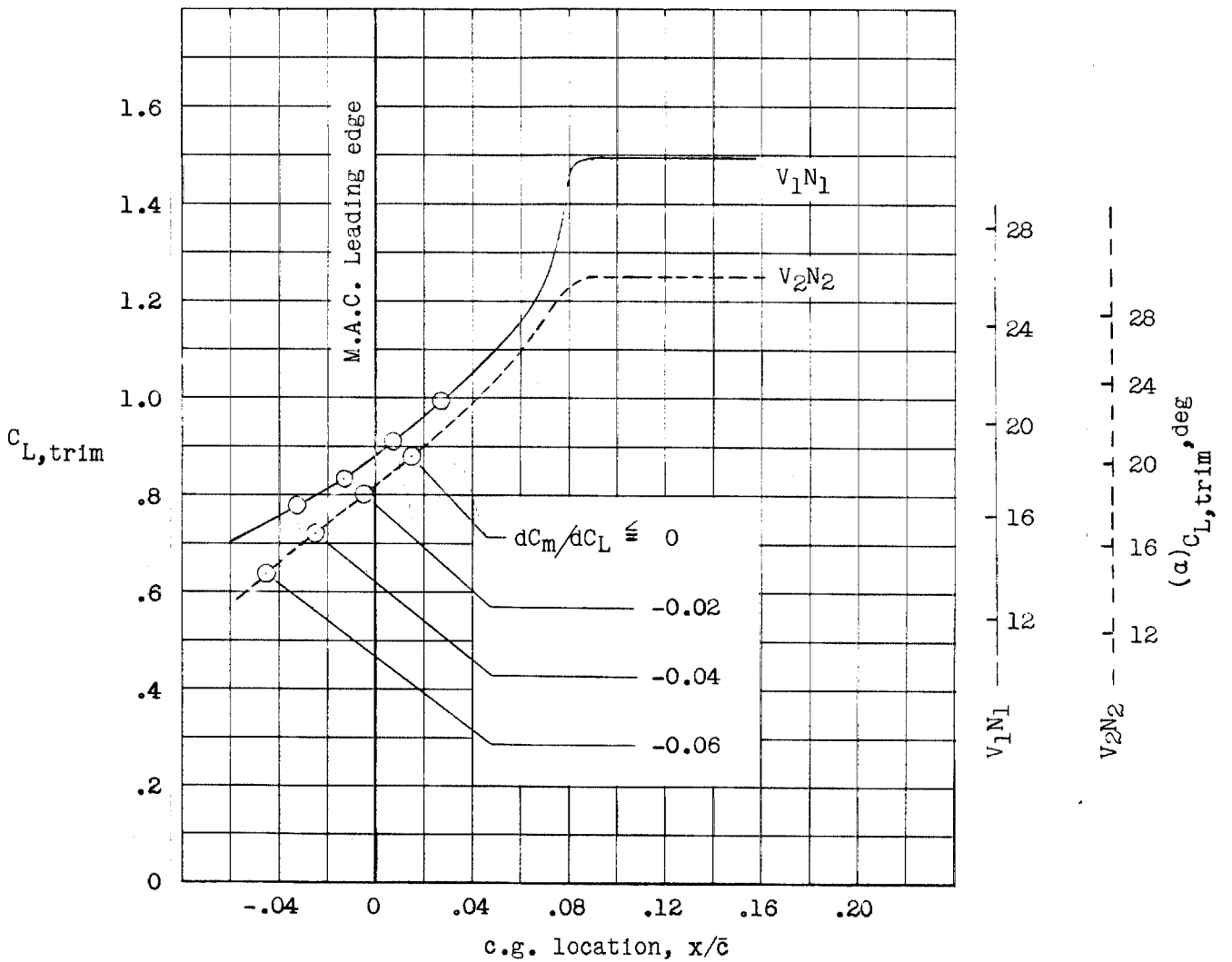

Figure 19.- Variation of maximum trim lift coefficient with center-of-gravity location of the model with the center vertical tail and with the twin vertical tails, $\delta_f = 0^o$.

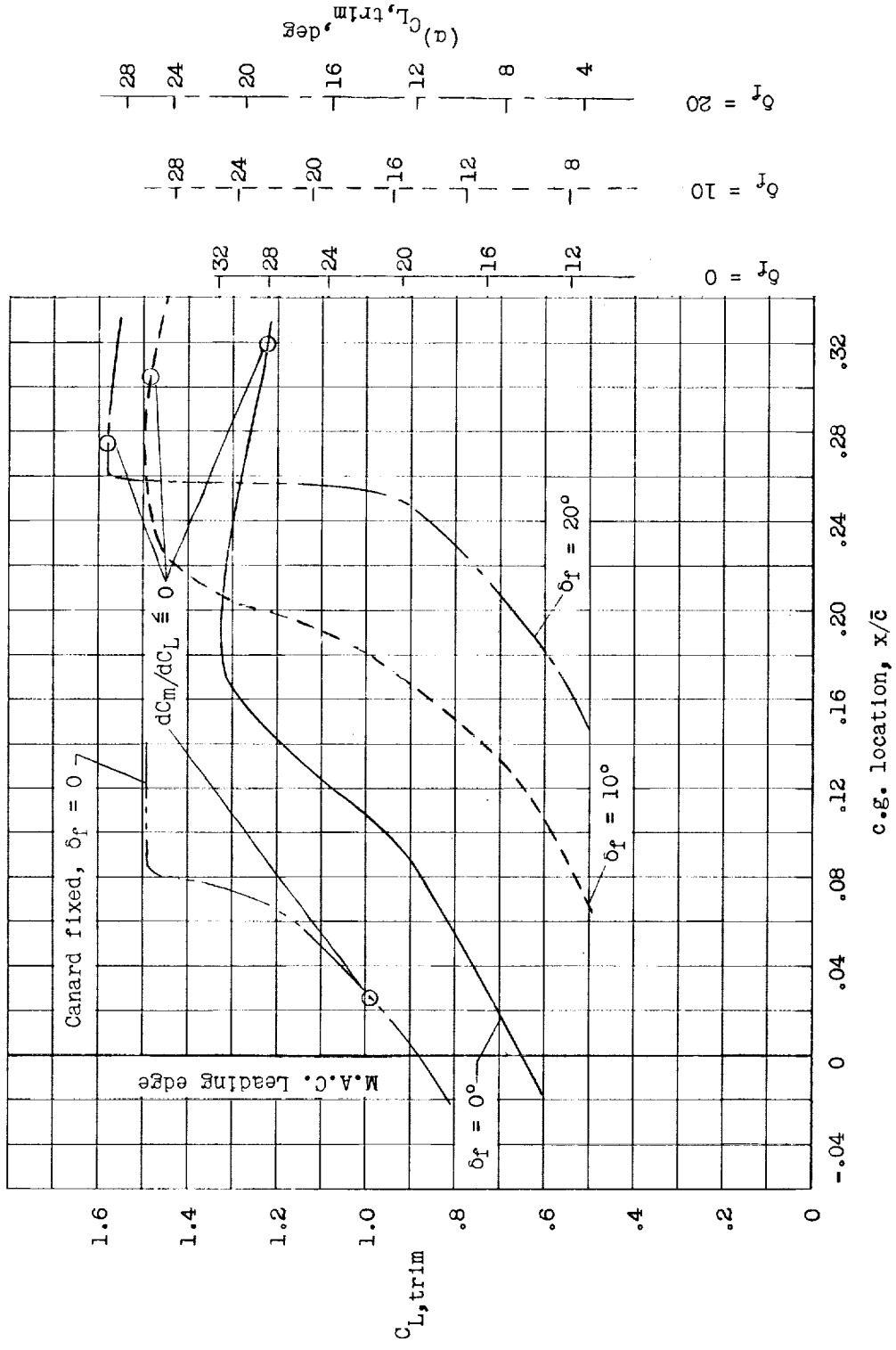

Figure 20.- Variation of maximum trim lift coefficient with center-of-gravity location of the model with an upright nose, center vertical tail, and the 0.20S canard fixed and free floating.

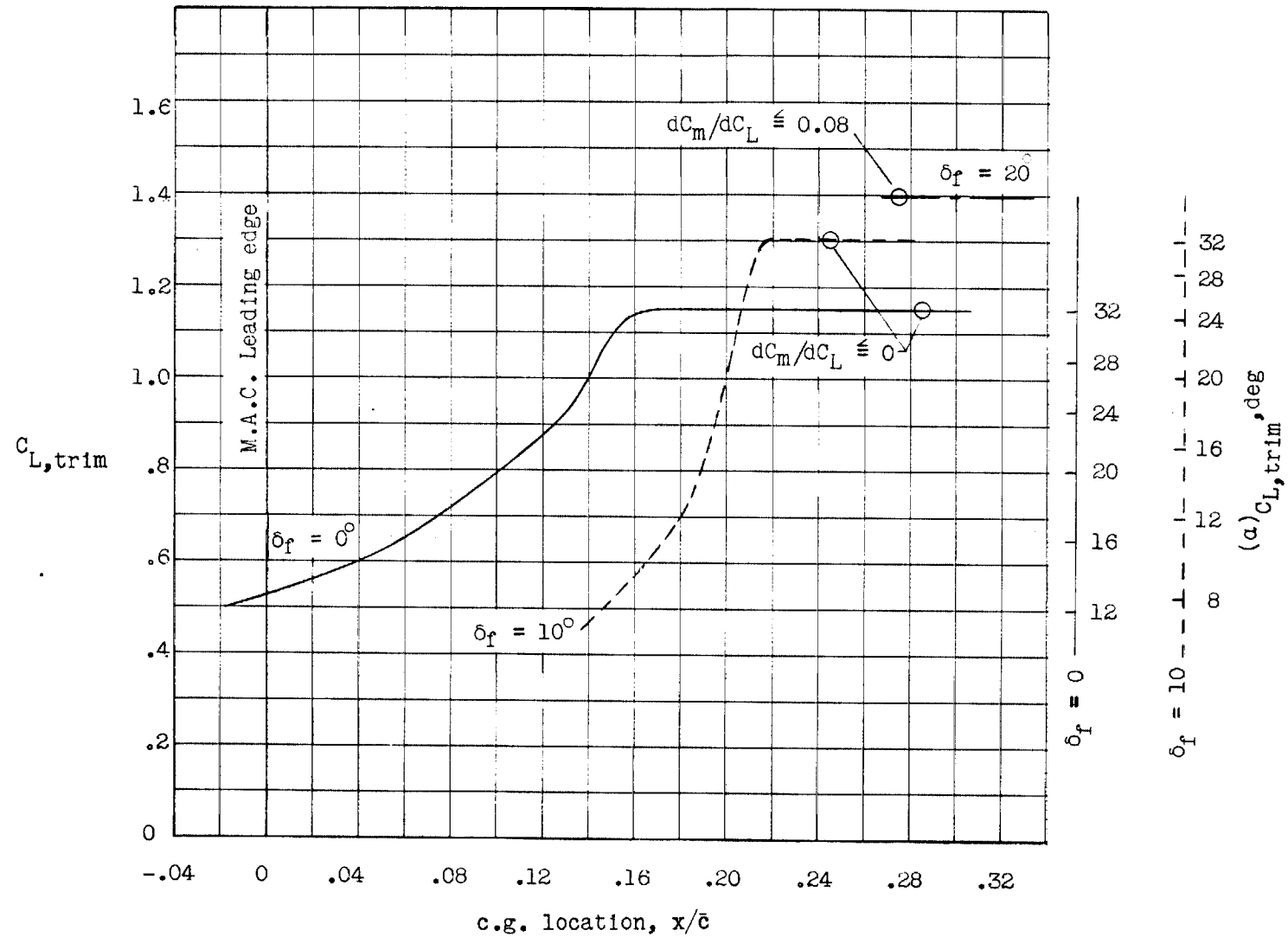

Figure 21.- Variation of maximum trim lift coefficient with center-of-gravity location of the model with twin vertical tails, nose inverted, and a 0.20S free-floating canard.

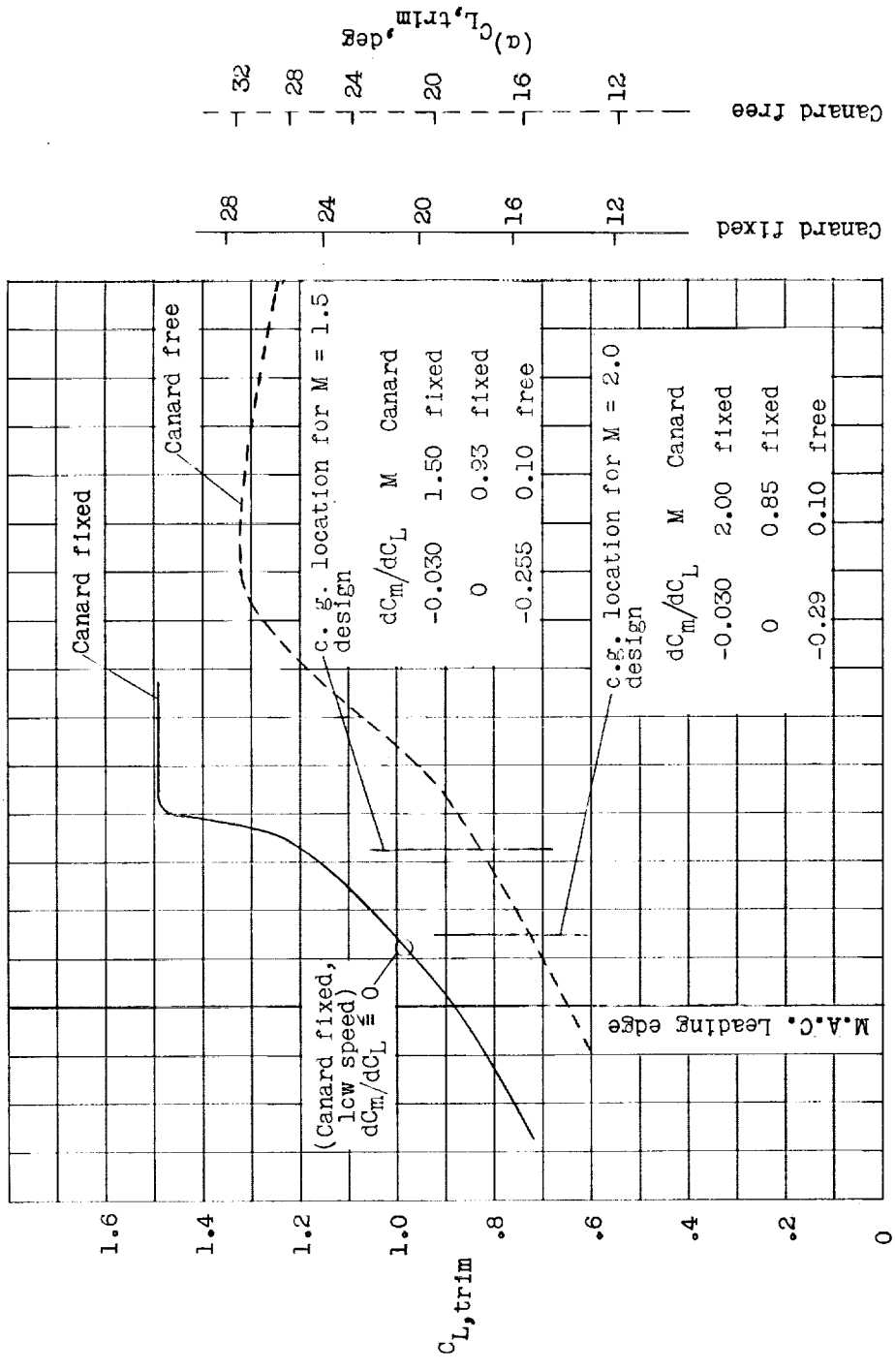

Figure 22.- Variation of maximum trim lift coefficient with center-of-gravity location of the model with canard fixed and free showing the center-of-gravity locations for two composite canard arrangements. Center vertical tail, nose upright, $\delta_f = 0^\circ$.

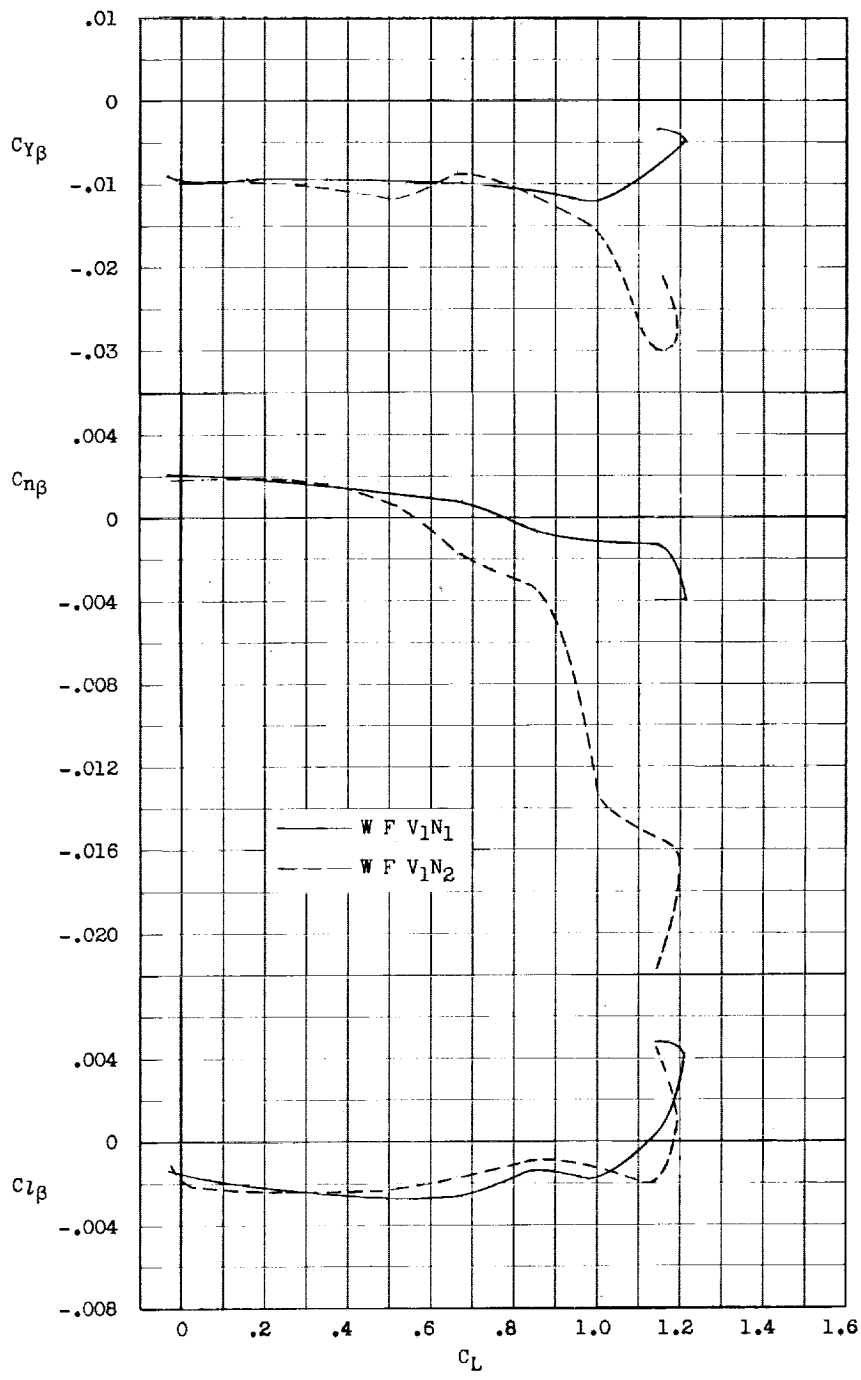

Figure 23.- Comparison of static lateral stability characteristics between the upright and inverted nose with canard off. $\delta_f = 0^\circ$; center of gravity at $0.275\bar{c}$.

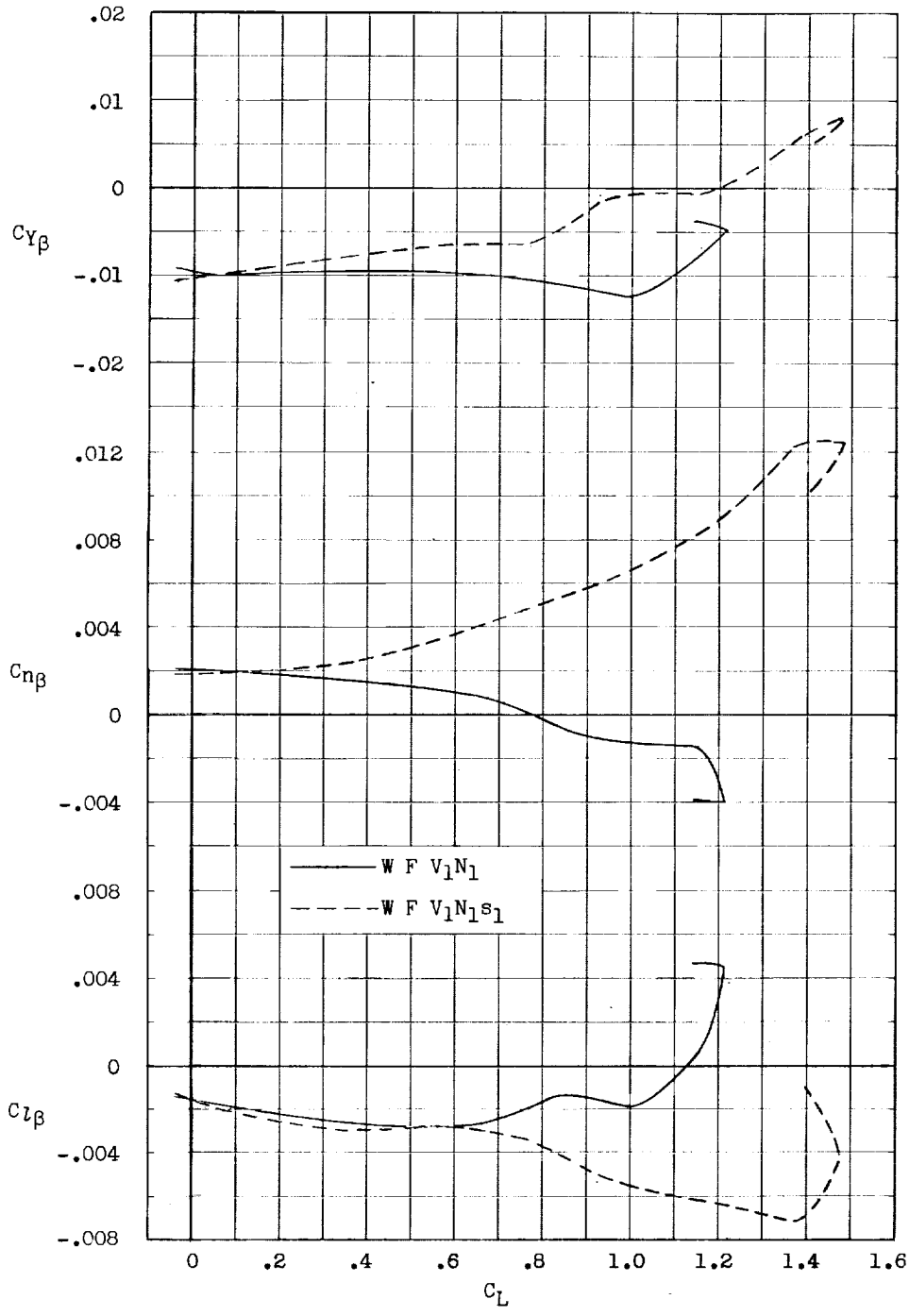

Figure 24.- Effect of nose strakes on the static lateral stability characteristics with the canard off and nose upright. $\delta_f = 0^o$; center of gravity at 0.275$\bar{c}$.

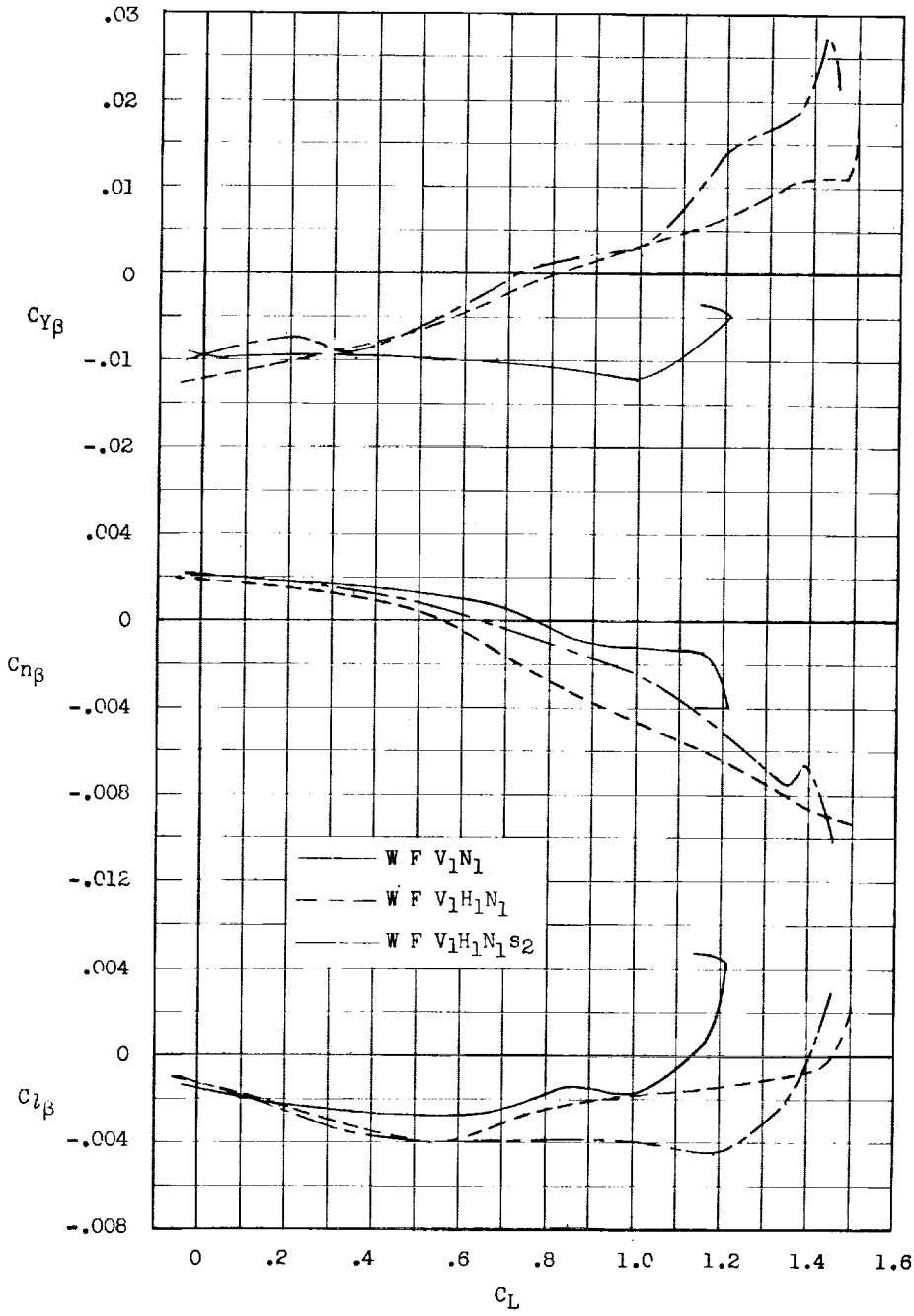

Figure 25.- Effect of nose strakes and the 0.20S fixed canard on the static lateral stability characteristics of a model having a center vertical tail and nose upright. $\delta_f = 0^o$; $i_t = 0^o$; center of gravity at $0.275\bar{c}$.

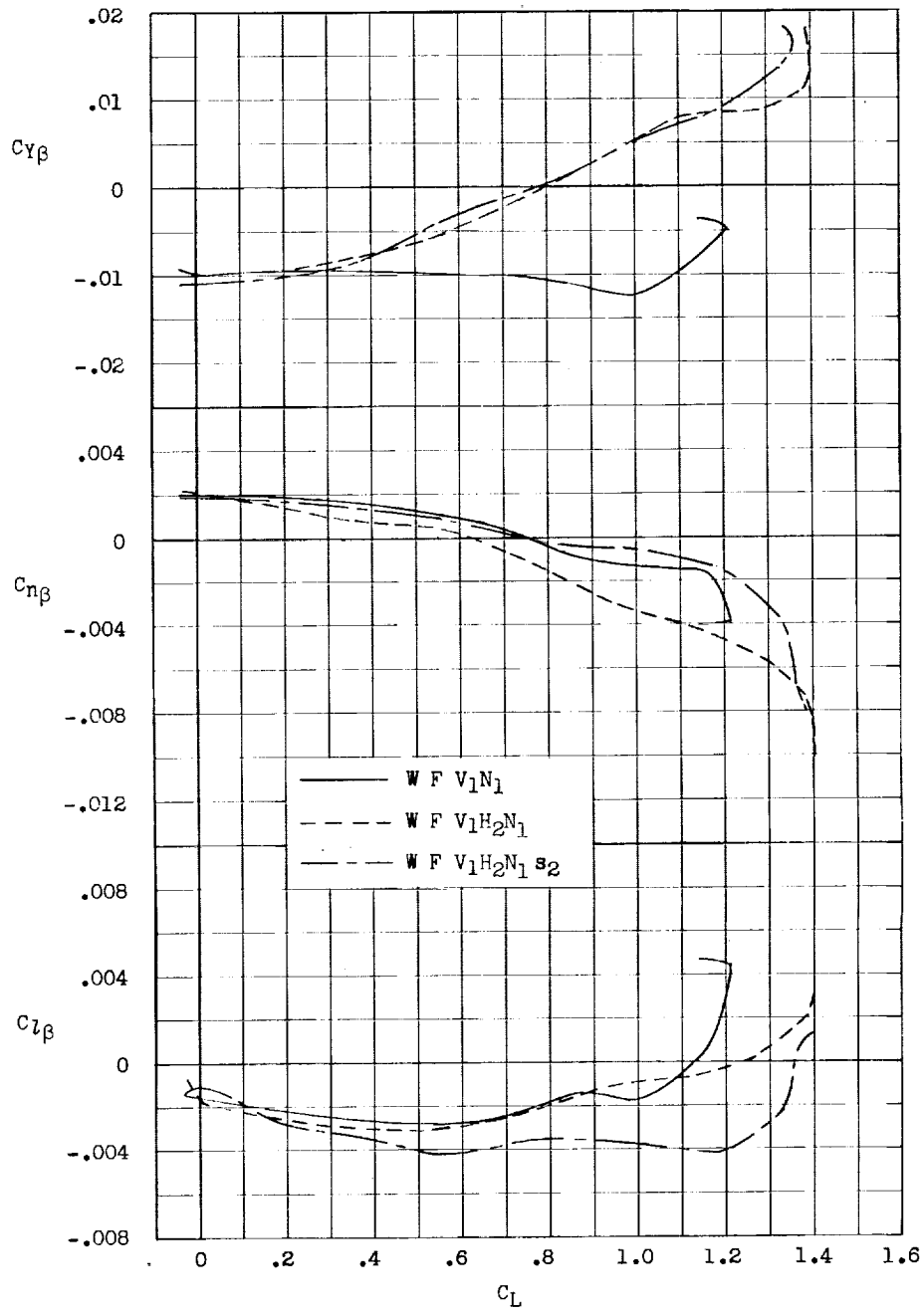

Figure 26.- Effect of nose strakes and the 0.15S fixed canard on the static lateral stability characteristics of a model having a center vertical tail and nose upright. $\delta_f = 0^o$; $i_t = 0^o$; center of gravity at $0.275\bar{c}$.

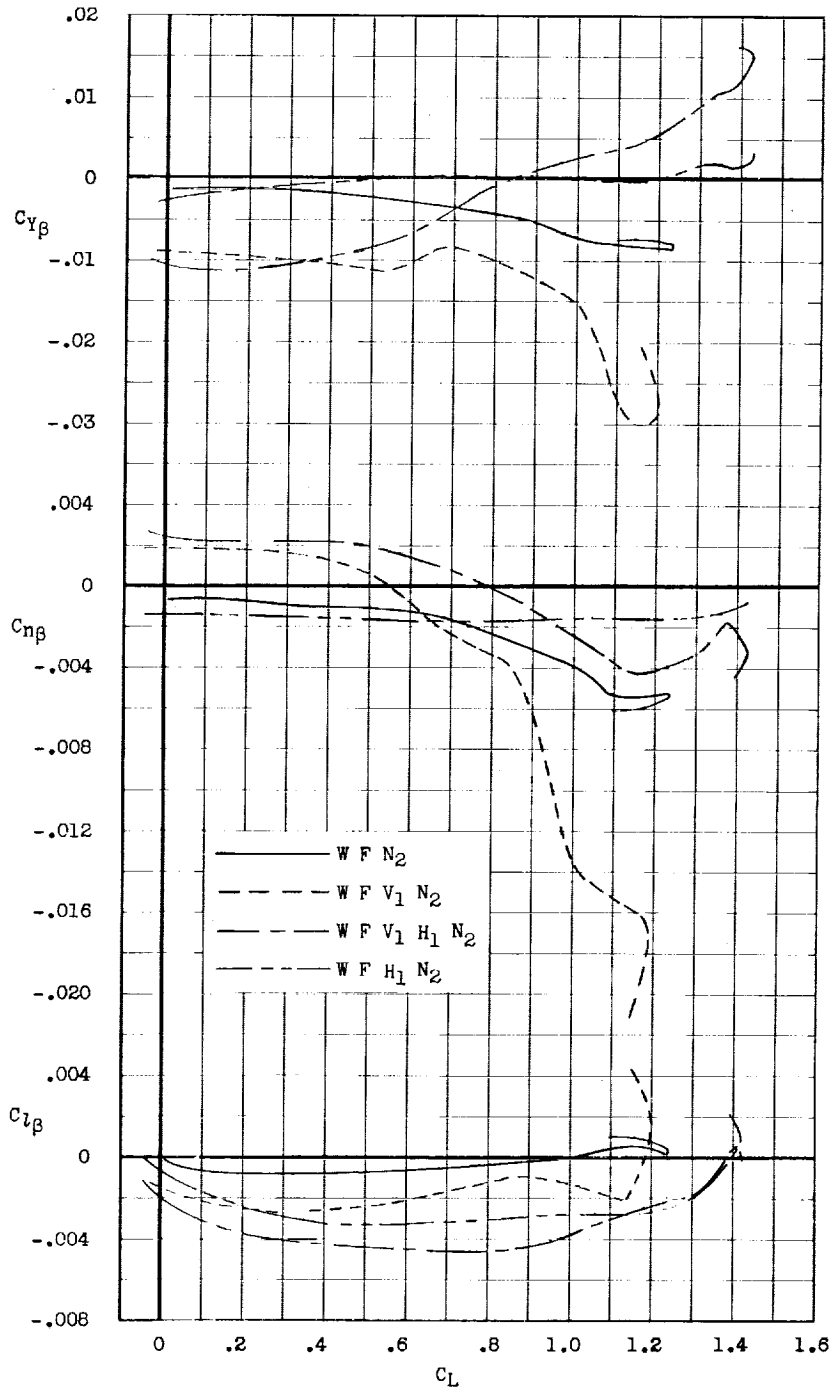

Figure 27.- Effect of the 0.20S fixed canard and center vertical tail on the static lateral stability characteristics of the model with the inverted nose. $i_t = 0^o$; $\delta_f = 0^o$; center of gravity at $0.275\bar{c}$.

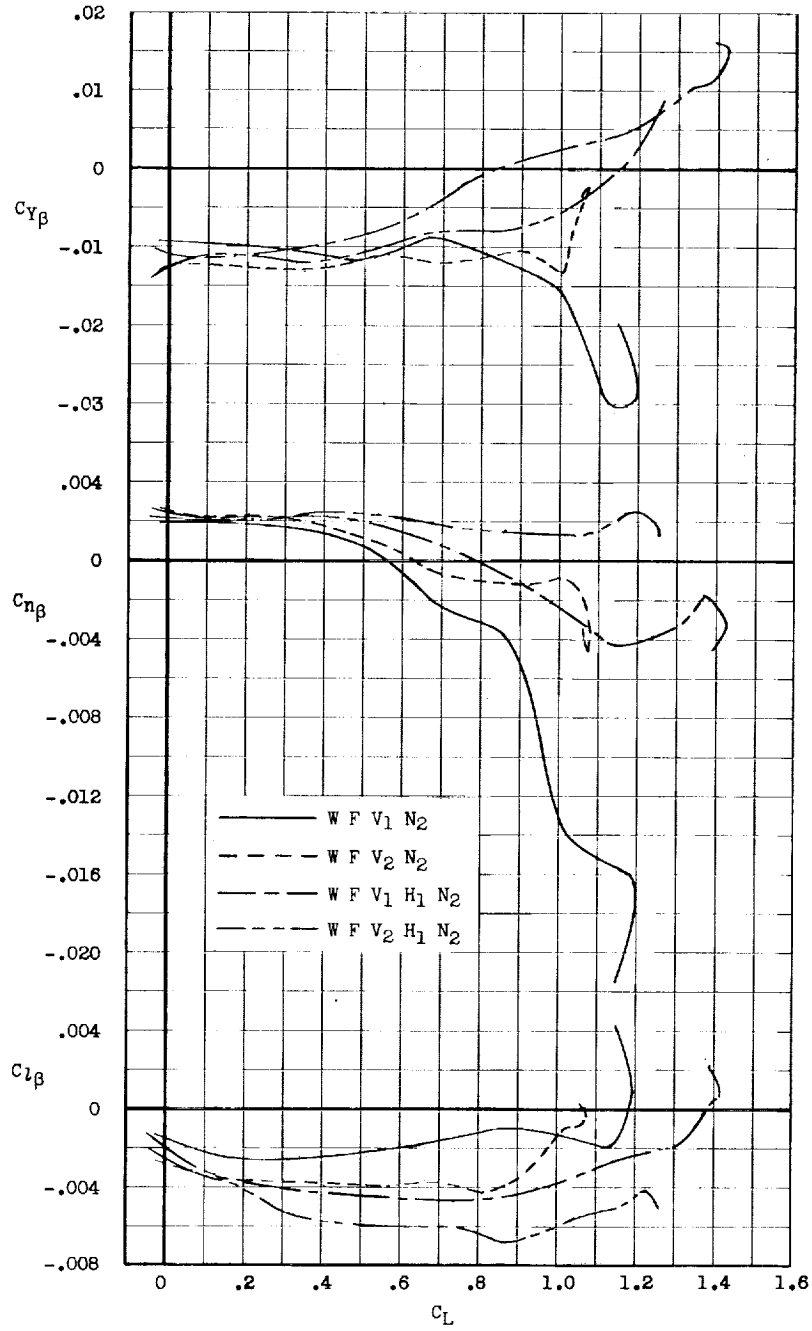

Figure 28.- Comparison of the static lateral stability characteristics of the model with the center vertical tail and twin vertical tails, nose inverted, and a 0.20S fixed canard. $i_t = 0^o$; $\delta_f = 0^o$; center of gravity at $0.275\bar{c}$.

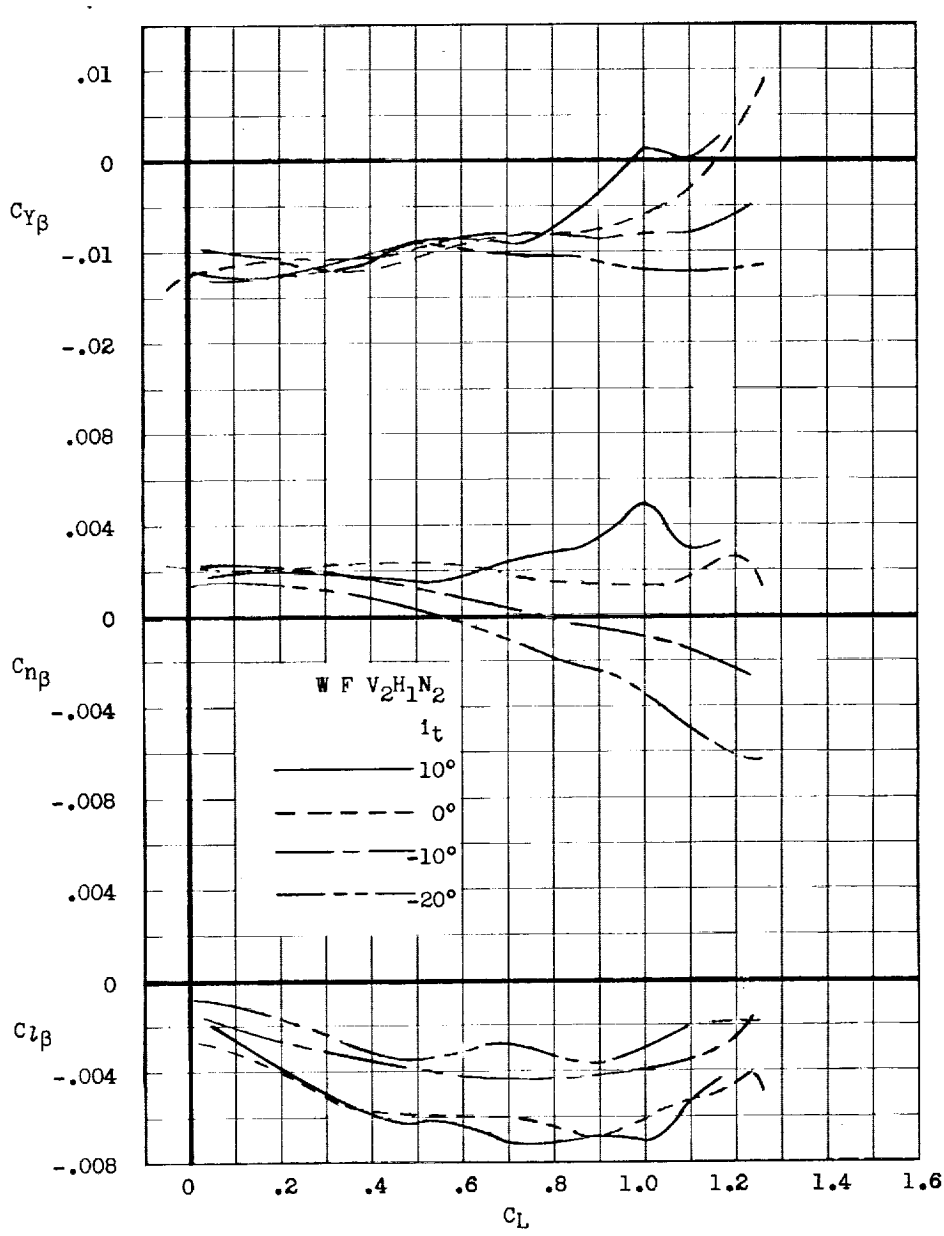

(a) $\delta_f = 0^\circ$.

Figure 29.- Effect of 0.20S canard incidence and full-span flap deflections on the static lateral stability characteristics of the model with twin vertical tails and inverted nose. Center of gravity at 0.275$\bar{c}$.

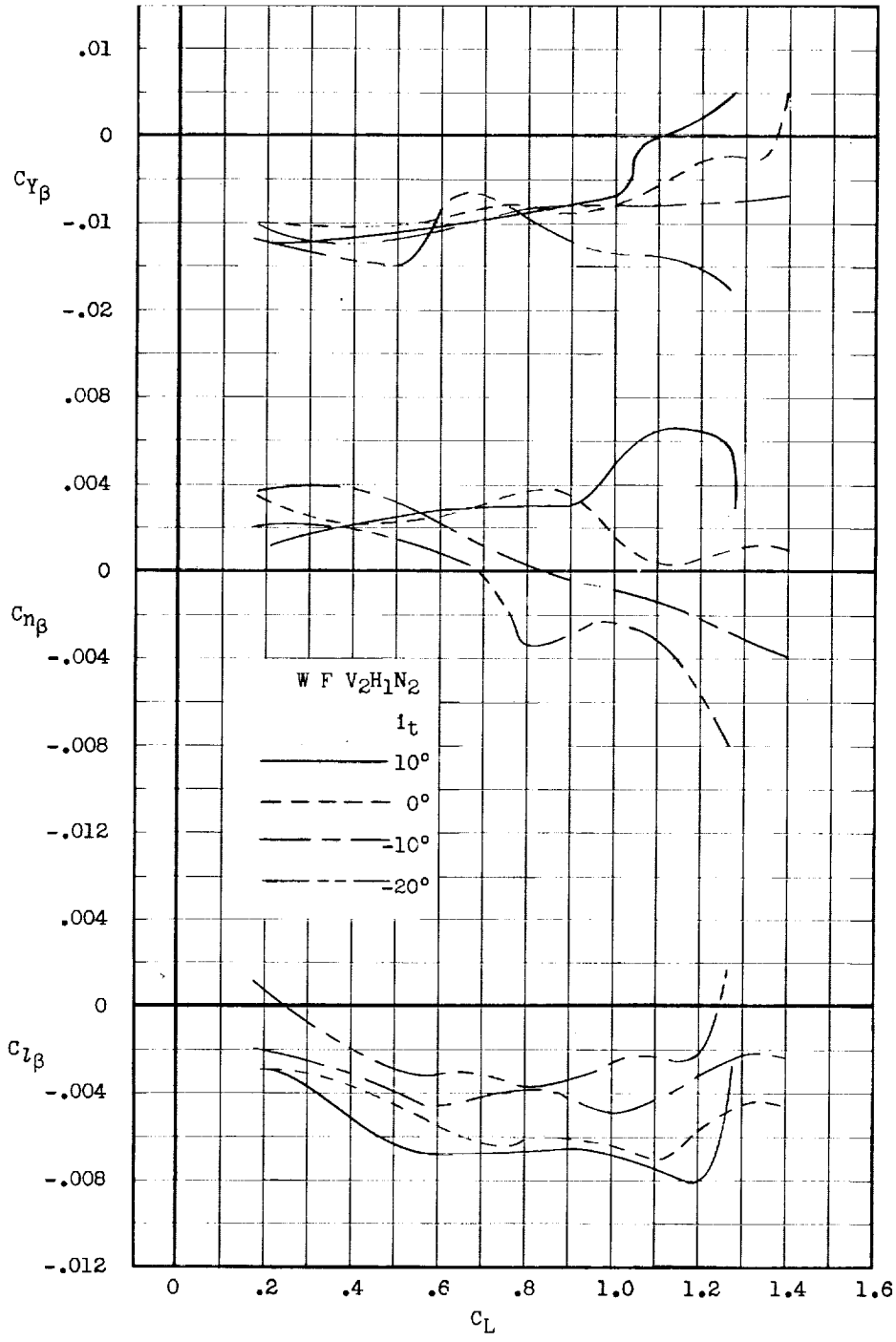

(b) $\delta_f = 10^\circ$.

Figure 29.- Continued.

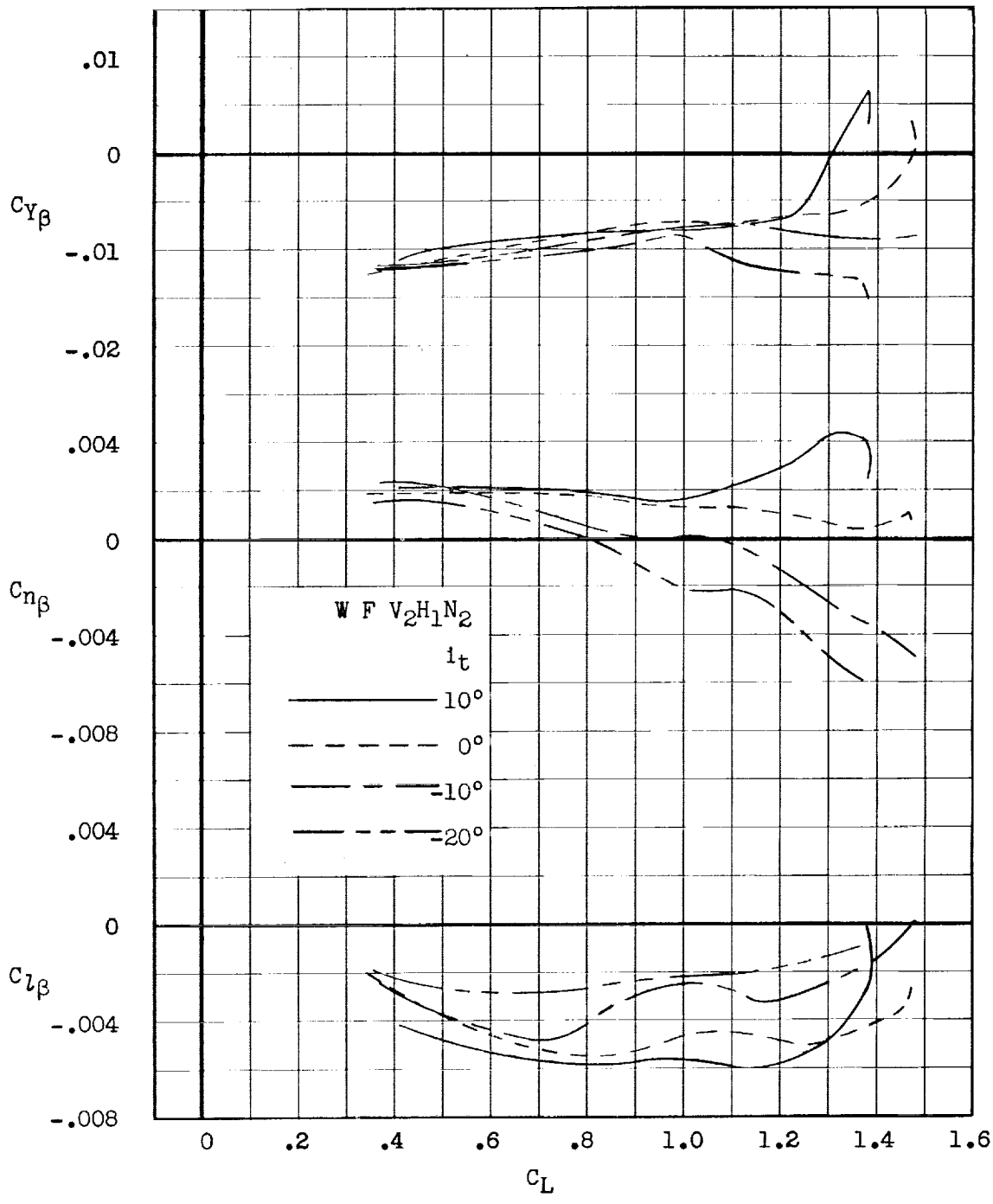

(c) $\delta_f = 20°$.

Figure 29.- Concluded.

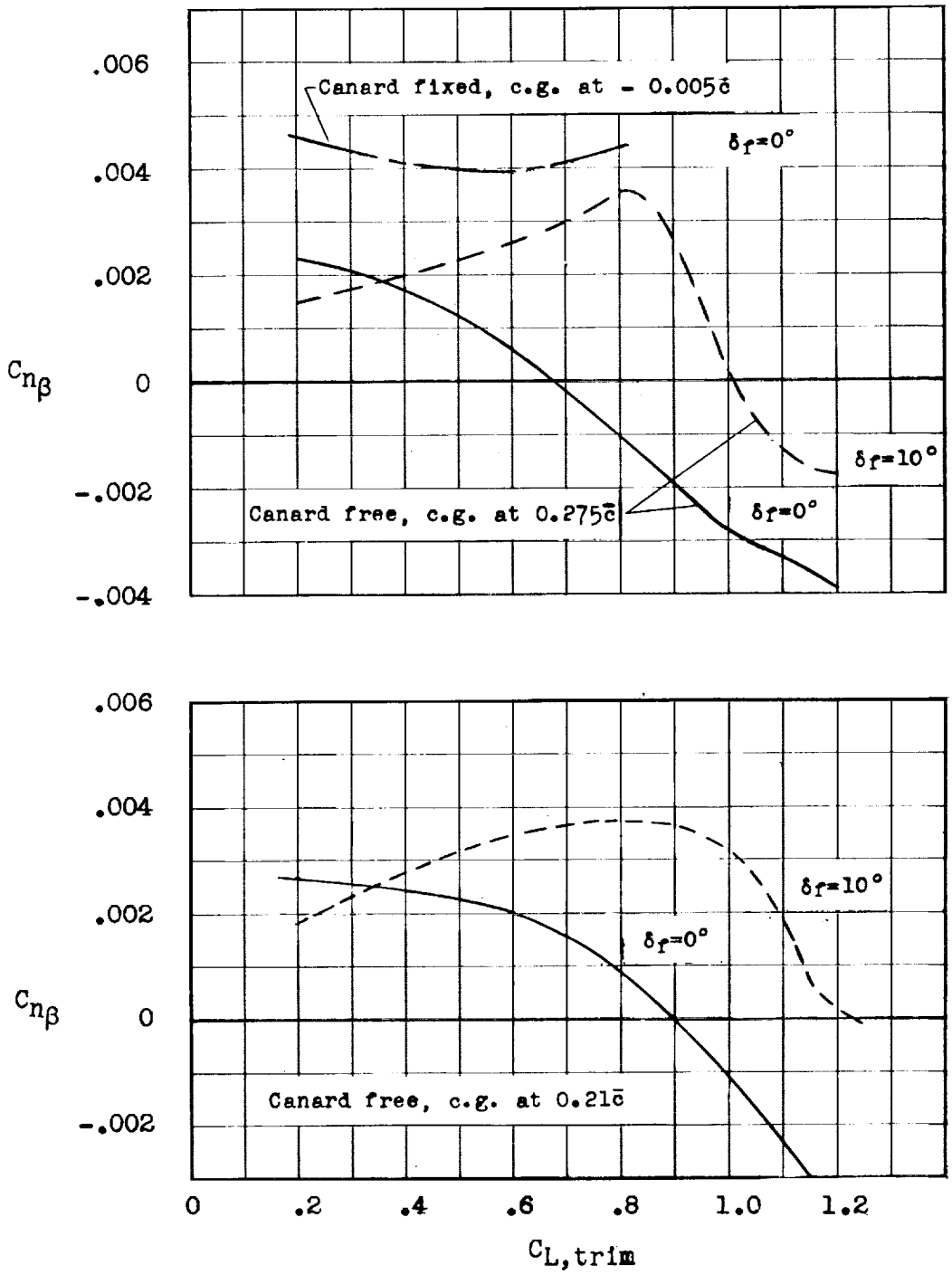

Figure 30.- Comparison of the directional stability of the model with twin vertical tails with the 0.20S canard fixed and free floating and nose inverted.

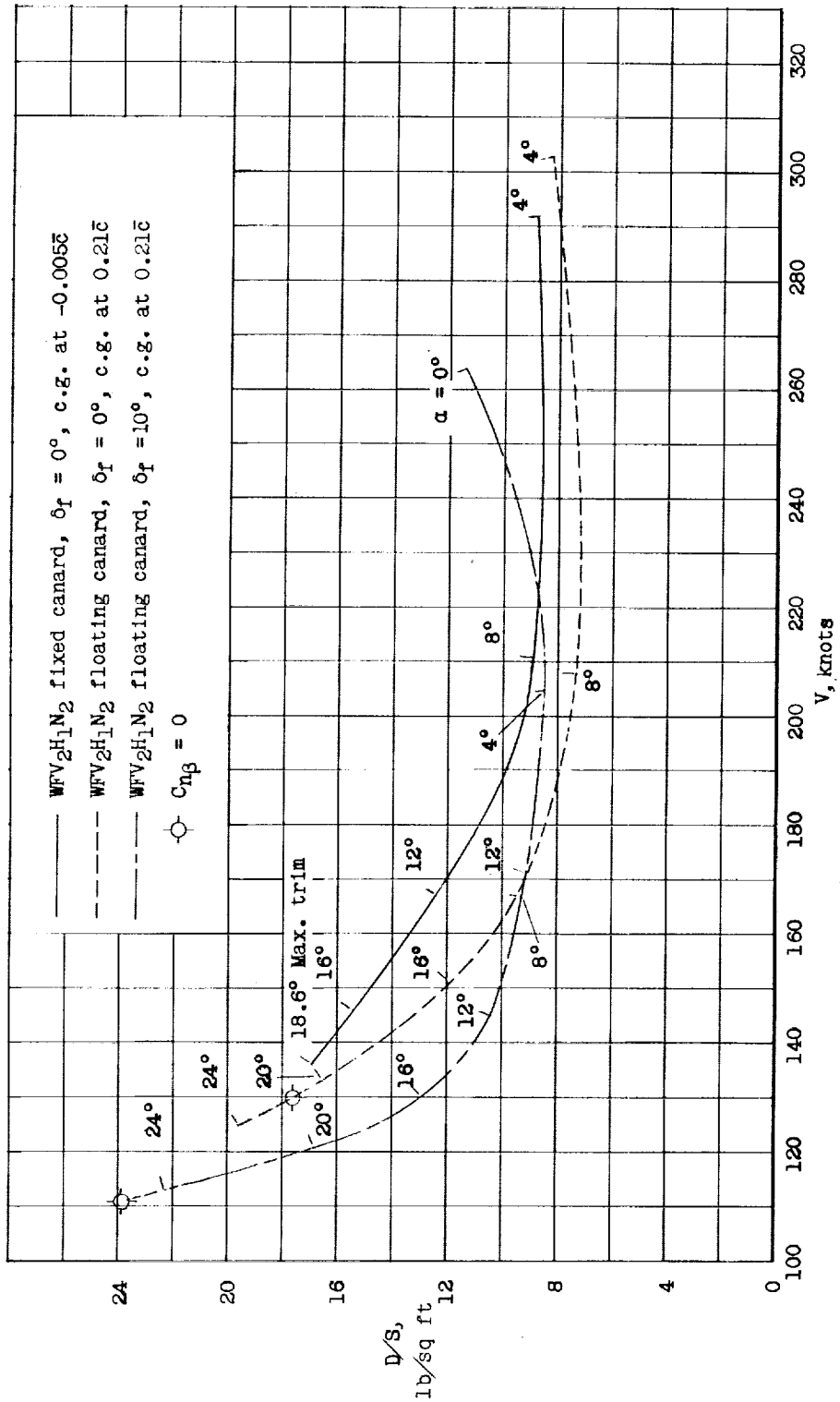

Figure 31.- Comparison of low-speed performance of a hypothetical delta-wing airplane with a fixed and free-floating canard. Wing loading = 50 lb/sq in.

NASA - Langley Field, Va. L-310